28 May 2017

Prof. Lars Kaleschke
Scientific Editor
The Cryosphere

Manuscript tc-2016-175

Dear Prof. Lars Kaleschke,

Please find attached the revised manuscript entitled *Estimating sea ice concentration in the Arctic Ocean using SMOS.* (Please note the title change.) This manuscript has been revised and improved based on the comments we received from you and the reviewers. These revisions do not change the main scientific results of the research reported in the manuscript.

We also attach the new version of the manuscript with marked changes (in blue color) with respect to previous version. Below we describe the revisions made to the manuscript and the response to the reviewers' comments.

Sincerely,

Dr. Carolina Gabarro
Barcelona Expert Center
Physical Oceanography Department
Marine Sciences Institute (ICM)
National Research Council (CSIC)
E-mail: cgabarro@icm.csic.es

Response to the Editor (Prof. Lars Kaleschke)

(*Original comments are shown in italics*; **Authors: responses in boldfaced font; number of lines and pages is from the track changes version or the manuscript.**)

The thematic comments of referee #4 reflect my main concerns: What is the advantage of the new method?

Authors: This comment has been addressed in the response to Reviewer #4. In essence, the main advantage of L-band observations is the significantly less sensitivity to atmospheric effects than observations from radiometers at higher frequencies, and to temperature changes than radiometers between 6-10 GHz. Furthermore, the effect of snow depth, which is an important contributor to the SIC error budget from higher-frequency radiometers, can be assumed to be negligible here. That is because this method relies on the use of angular differences (AD) of only vertical polarization (V-pol) observations and, as shown my Mass et al. (2015), the effect of snow depth is observable at horizontal polarization (H-pol) but not vertical. Moreover, the method presented here is robust because uses a maximum likelihood estimator (MLE) to invert for sea ice concentration (SIC) parameters. This is also a new feature of this method, and could be beneficial for data obtained from other radiometers. All in all, as Reviewer#3 also pointed out, this is a new independent method that can help cross-check SIC results obtained with other methods.

How can the interference between thickness and concentration be resolved?

Authors: This question has also been addressed in the response to Reviewer #4. We have removed the single comment there was in the original manuscript to a suggestion of attempting the simultaneous estimation of SIC and sea ice thickness (SIT). We realize this is an important but also difficult problem that deserves some serious research. The comment was largely motivational, but has now been dropped.

One main parameter in question is the PD which is also used for the retrieval of ice thickness, see Huntemann et al. (2014) equation 4. This usage seems to be in strong contrast to your results shown in Fig. 5 which suggest only a weak dependency of PD on thickness.

Authors: The thrust of this study is a new method for SIC not SIT retrievals. Figures 10 and 11, which are derived from observations, suggest that there is some PD sensitivity to ice thickness and that SIC differences are associated with regions of thin ice. Figure 5 estimates are derived from a theoretical model that incorporates various simplifying assumptions and nominal model parameter values. Like with most models, while being useful they also have their limitations. We feel there is no need to discuss methods for

retrieval of SIT including Huntemann because our study focuses on SIC, not on SIT retrieval.

The model assumes dry snow but the algorithm is applied during the melting period. An extended discussion on the Summer period may perhaps help to show the advantage of SMOS for ice concentration retrieval. You state that there are no validation data before the launch of SMOS to calculate uncertainties. But you could make comparisons to other independent ice concentration estimates, e.g. using high resolution optical data in cloud free areas.

Authors: It should first be clarified that our algorithm for SIC retrieval is fully empirical, no assumptions are made on the type of snow. The assumption of dry snow is only made when discussing theoretical models, which are discarded for the construction of the algorithm.

The comment is nevertheless appreciated, and we take good note for future work. In our response to Reviewer #4 on this topic, we indicated that a comparison with optical imagery would help for validation purposes of SMOS SIC during summer periods but that such study is beyond the scope of this manuscript.

To improve the reproducibility I place emphasis on the comments of referee #2 who asked for the model equations.

Authors: This has been done, as indicated in our response to Reviewer #2.

Regarding the structure I recommend to split discussion and conclusions. The title should be changed according to the suggestion of referee #3.

Authors: The sections have been split, the title changed, and the manuscript edited and proofread.

Response to Reviewer #2 (anonymous)

General Comments:

Sea ice concentration observations are a highly relevant topic. In summer, sea ice concentration products have typically higher uncertainties compared to winter. Extending the frequency range of passive microwave retrieval algorithms to lower frequencies such as L-band, has the potential to lower the overall uncertainties of sea ice concentrations. The Manuscript is well written and combines theoretical and empirical aspects to derive sea ice concentration from multi angular observations from SMOS. The presented algorithm includes an estimation of uncertainties of sea ice concentration retrievals and is compared a sophisticated operational sea ice concentration product.

Authors: We thank the reviewer for the positive comments and summary.

Specific Comments:

The manuscript is suitable for publication in The Cryosphere after addressing the following specific comments:

P2, L6: remove "AMSR-2 and"

Authors: Done.

P3, L27: how can it happen that the incidence angle range is not fully covered within three days? It should be mentioned in the manuscript if also extrapolation is done or not. "interpolate TB to locations" here is misleading as it sound like interpolating spatially and not in TB-incidence angle space.

Authors: The sentence has been modified for improved clarity, in line 112, page 4.

P4, L16-17: all "self-emitted"□"emitted"

Authors: Done in line 137, page 5. In fact, the "self-" had been added on a suggestion from a previous reviewer.

P5, L8-10: remove parenthesis

Authors: Done.

P5, L12: "models" -> "cases"

Authors: Done.

P5, L12: remove "larger"

Authors: Done.

P5, L18: remove "spontaneous"

Authors: Done.

P5, L11-13: Actually the water under sea ice has a contribution to the emissivity, as you can easily calculate with your model, but you mean probably that the emissivity is not getting higher with increasing ice thickness from about 60cm, i.e., the signal saturates. Please rephrase the sentence. (see also comment on P6, L25)

Authors: That is correct, the emissivity does not further increase for ice thicker than about 60 cm because of attenuation. The sentence has been rephrased in line 180, page 6.

P5, L23: Snell's law describes the propagation direction inside a medium with respect to its permittivity and does not describe transmissivity/emissivity.

Would be good to have either a reference (maybe Schwank et al. (2015)) or more explanation.*

Authors: Sentence rephrased, and reference added, in line 190, page 6.

*P5, L29-30 (Eq. 3): Burke et al. (1979) actually does not make the step to expand the multiple reflection to the binomial series. So the source of the Equation could be Ulaby (1981)** Eq. 4.163, or derived from Ulaby (2014). A follow up on this equation is also useful as most of the terms disappear or become much simpler once you assume negligible attenuation in the snow. Also the later used water layer is not included in this equation.*

Authors: The reviewer is correct, it is Ulaby and not Burke who expands to multiple reflections in the case of three media. We have changed the text accordingly, in line 200, page 7.

P6, L5-6: remove "conducting". For sure it is also true for a conducting medium but you stated the alpha for low-loss-medium, means no- to low- conducting material. Also the penetration depth is not used further in the document, so the sentence may be removed.

Authors: Removed "conducting." About the skin depth, we think it will help the reader the general to better grasp the meaning of the equations, thus kept it.

P6, L7: The dry snow dielectric properties are discussed twice, here and in P5, L22-It is probably good to put this together for consistency.

Authors: Done. Now the snow discussion is in lines 184-194, page 6.

P6, L22: Equation for the four layer model is missing.

Authors: **Included, as Eq. (9), in page 7.**

P6, L25: The surface emissivity of seawater is not a relevant quantity for the transmissivity of radiation from seawater under the ice into the ice layer. The boundary between seawater and sea ice has a different reflectivity compared to the boundary between seawater and air because of the different permittivities of ice and air. I suggest to just remove the mentioning of the emissivity of sea water and start with "The net effect ...

Authors: **Accepted and implanted, in line 148, page 8.**

P8, L20-23. The variation of a quantity with another within a multi dimensional space depends on all other variables in case they are not dependent nor correlated. However, Table 2 shows only a single value for each quantity. Please give more details on how these values were obtained.

Authors: **To compute the sensitivities of the indices (Tb, PD, AD) to several parameters we use the range of values of each parameter, and the rest of the variables are set to the values in page 5 line 9 - 10. It is now specified in the text, line 320, page 10.**

References:

*Schwank M, Mätzler C, Wiesmann A, et al. Snow Density and Ground Permittivity Retrieved from L-Band Radiometry: A Synthetic Analysis. IEEE J Sel Top Appl Earth Obs Remote Sens. 2015:1-14. doi:10.1109/JSTARS.2015.2422998.

**Ulaby FT, Moore RK, Fung AK. Microwave Remote Sensing: Active and Passive. Volume 1 - Microwave Remote Sensing Fundamentals and Radiometry. Artech House Publishers; 1981.

Response to Reviewer #3 (Dr Mohammed Shokr)

General Comments:

The manuscript introduces a new algorithm to retrieve sea ice concentration in the Arctic region based on radiometric observations from the L-band SMOS, with its multi-viewing angles. It uses the Maximum Likelihood criterion with input distributions of a couple of radiometric indices, assuming Gaussian distributions with mean and standard deviation obtained from model and observation findings.

The idea is interesting, the study is scientifically warranted and it is an appropriate continuation, with a remarkable progress, of the limited number of similar studies using SMOS in the past 8 years. I would recommend publication and certainly commend the authors on their effort. However, one should keep in mind that the challenge of estimating SIC from remote sensing data remains.

In most studies, sea ice is treated as one entity. Yet, in nature it is manifested in several types with large diversity of physical properties that may lead to consider it as different entities. Thin ice, seasonal ice, perennial ice, summer ice, etc. are different "creatures" within the realm of sea ice; let alone snow-covered ice under different metamorphosed snow conditions that lend itself to different radiative properties, even under the passive L-band radiometry. Given this concept, I would be cautious when considering SIC algorithms trying to approximate the wide range of ice properties into a single set.

Authors: We thank the reviewer for his summary and praise of the study.

With this in mind I am not comfortable with the title of the paper that groups all ice types under one phrase "sea ice in the Arctic Ocean", but I guess nothing can be done here! But it would be more appropriate to use the word "Estimating" in the title instead of "Measuring" since we don't really measure SIC.

Authors: Changed the title from Measuring to Estimating.

The method adds to the tools of estimating ice concentration from microwave data. One advantage of having different methods is to be able to perform cross-checking. This is important because there is no reliable "truth" data against which we can evaluate each method. All methods suffer from errors and the only way to approach the "truth" is by cross-checking. For example, the current study performs the validation by comparing results against maps from OSI-SAF. But the latter, much like any other operational ice maps, may not be considered truth data either.

Authors: **We fully agree that the method presented here will enable independent evaluation of results obtained using other methods. Cross-checking of results is a tenet of the scientific method.**

Another concern is about a sentence in the Abstract; "We find that sea ice concentration is well determined (correlations of about 0.75) when compared to estimates from other sensors such as the Special Sensor Microwave/Imager (SSM/I and SSMIS)." Retrieval of any parameter from remote sensing data is associated not only to the sensor characteristics but also to the retrieval method. I believe the method used in this study is new, so if there are other method using L-band then the authors can do comparison. To keep the above statement, the authors should qualify it; namely to say correlate well with other passive microwave – but under what condition (when and where). I think it should correlate well with other sensors over mature Arctic sea ice in winter. Other than that I don't think the correlation would reach 0.75.

Authors: **We have changed the sentence to be more explicit about the correlation, now specifying both the elements involved in the comparison (i.e., MLE/SMOS vs OSI-SAF/SSMIS) as well as the span both in the time (one year, 2014) and space (pan-Arctic) domains. The *changes are done in lines 9-14, page 1 from the track change version of the manuscript.***

To the best of our knowledge, this is a completely new approach to SIC estimates in that this is the first time that L-band observations are used to estimate SIC and also the first time that a MLE criterion is used to retrieve SIC.

Specific Comments:

A few suggestions for corrections are listed below. It would be nice if the authors consider them while preparing the final submission.

Page 4 Line 21: correct the sentence to be "Hereafter we will use TB to refer to surface brightness temperature, for simplicity"

Authors: **Done, *line 140, page 5.***

Page 4 Line 25: correct the sentence to be "is the ratio between reflected and incident radiation"

Authors: **Done, *line 144, page 5.***

Page 5 Line 4: no need to mention the refractive index (n); this is for optical remote sensing but here we deal with microwave.

Authors: **Done, *line 145, page 5.***

Page 5 line 6: the sentence "The nonlinearity is an advantageous property for remote sensing …" is not explained. How? Also it has no relevance to the text before it. The authors may remove it.

Authors: **Removed, *line 155, page 5.***

Page 5 Line 7: if Fig. 2 is for the L-band please mention that in this line or in the figure caption. Also, while the authors mentioned the seawater and sea ice parameters that are used in equation 3, they did not mention the snow parameters. Here they have to be careful because it is difficult to characterize the snow by a single temperature value as it is highly responsive to the air temperature. Even for dry snow, it can be lossy because the salinity at the snow base is usually higher than 0; it can be as high as 20 ppt or higher as shown in many studies.

Authors: **Changed both the text and figure caption to indicate this is L-band, and also added the snow values used.**

On the snow comment, Schwank et al 2015 confirms that at L-band the imaginary part of the dielectric constant is very small compared with the real part, and stats that it can be neglect in the model of snow dielectric constant. This has been clarified in the manuscript in lines 182-190, page 6.

Page 5 line 23: "dry snow still has an effect in (make it "on" not "in") emissivity that changes with the angle of incidence according to Snell's law". Snell's law is about the angle of refraction, nothing to do with the emissivity.

Authors: **Thanks, we have modified the text accordingly, in lines 189, page 6**

Page 6: in the set of presented equations I think one equation is missing; that is the one that determines the reflectivity from the ice surface in terms of its dielectric constant (i.e. Fresnel equation). This should be inserted before equation 5.

Authors: **Inserted, see Eq. (3) in page 5**

Page 7 line 7: close the bracket after (resulting from ….unknown physical parameters).

Authors: **Done**

Page 7 line 10: something wrong in the sentence "… among conditions such as deletedwhen a phase change …"

Authors: **Done**

Page 7: just wonder why didn't you use the polarization ratio instead of the polarization difference? The former is more common and it eliminates the dependence of the brightness

temperature of the physical temperature. I am not suggesting to change the present scheme but an inclusion of a sentence to explain why PD and not PR would be useful.

Authors: We have preferred to use PD instead of PR, since we have verified that the former has a larger dynamic range than the latter. Given the SMOS measurement errors a parameter like PD with a relatively large dynamic range is more suitable for SIC retrieval purposes. This is now clarified in the text in lines 278-280, page 9.

Page 7 Line 25 "we will use tie points as ground truth estimates of sea ice concentration". What does that mean? Tie points are used to estimate ice concentration based on a set of algebraic equations.

Authors: Modified in line 284 page 9.

Page 8 Line 7: just a comment on Figure 5, it is good to see the model confirms what we know – that Tb, not PR or PD can be used to estimate ice thickness. The latter are good for estimating ice concentration.

Authors: Good remark, we have added a sentence to that effect "Compared with TB, the total variation of both AD and PD with ice thickness are significantly smaller and, therefore, are better suited to estimate ice concentration" in line 209 page 10.

Page 9 Line 3: the statement "AD is the most robust index to retrieve SIC, slightly better than PD, and significantly better than TB, as TB is highly sensitive to ice thickness variations" may need some more thought. The fact that TB in the L-band is sensitive to the thickness has no relevance to its robustness in retrieving SIC of total ice (i.e. concentration regardless of ice thickness), hence the above statement may not be accurate. As mentioned in the text, the L-band has problem in estimating SIC only when the ice is thin (a few centimeter) and becomes partially transparent to the L-band. I think what can be used to comment on the high value of the propagated error in Table 3 when TB is used is the fact that the variability of TB is quite high with the thickness parameter (unlike the temperature and salinity) because of the large penetration of the L-band, and may not conform to the Gaussian assumption.

Authors: Thanks, this is a very interesting remark. We have introduced a sentence on the text to account for this, in line 338 page 11.

Page 12 Line 1: change the word "replacedmoenthsepochs".

Authors: Done.

Page 12 Line 1: when talking about Fig. 10, the given information is expected, nothing new. I would prefer seeing Fig. 10 generated for data in winter months. Ice in Laptev and Kara seas remains thin during winter. The region remains a marginal ice zone throughout most of the

freezing season. So, I believe that we will see the same difference during November and December as we see it during the period 2-5 November shown in Fig. 10. But it is interesting to confirm that. The authors may refer to a publication about thin ice in the Arctic titled "Interannual variability of young ice in the Arctic estimated between 2002 and 2009".

Authors: The purpose of Figure 10 is to show that the main difference between using the AD index vs the AD plus PD indices occurs in regions known to be covered with thin ice, not (at least yet) to turn it around into a possible analysis tool for locating regions of thin ice. We have added the proposed reference and a sentence explaining the situation observed by the reviewer (lines 502-507, page 16).

However, we add the figures the reviewer is asking for, for his information:

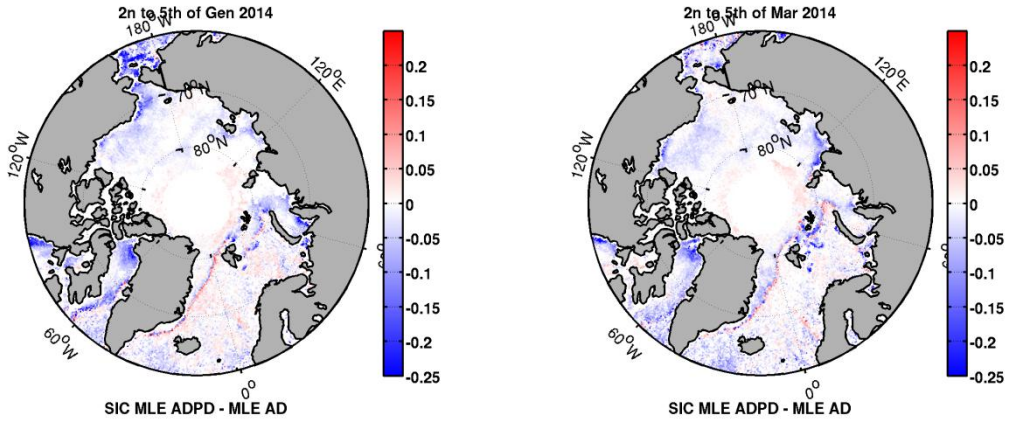

Page 13 Line 5: Same argument applies here. The text says "… for some days in November, the month of maximum extension of thin young ice". My argument is that this statement applies to ice extending west through the Beaufort Sea" but not in the Laptev and Kara Seas area, where thin ice cover continues to exist in winter.

Authors: A comment and the reference have both been added.

Figure 6: in the caption it should be mentioned that the values for the ice are coming from multi-year ice (as mentioned in the text).

Authors: Done.

Figure 10: I believe that the difference of SIC is presented in scale of tenth concentration. Please indicate that in the caption. The advantage of this figure is not limited to what is already described in the paragraph. It also marks the area of highly dynamic and ice reproduction, which, again not limited to November.

Authors: Agreed and done.

Finally - the phrase "tie-point regions" is confusing. Better use "regions for generating tie-points"

AUTHORS: Agreed and done.

Response to Reviewer #4 (anonymous)

General Comments:

The authors develop a new algorithm to retrieve sea ice concentration from the L-Band SMOS measurements at 1.4 GHz. At 1.4 GHz, the influence of the atmospheric properties on brightness temperatures is very low and, additionally, SMOS provides full-polarized measurements at different incident angles. Due to a higher penetration depth, information about the sea-ice thickness can be retrieved in addition to sea-ice concentration. Ideally, the method here is a first step to combining sea-ice concentration (SIC) and sea-ice thickness measurements from the same place at the same time.

For their new SIC retrieval method, the authors take advantage of the special features provided by SMOS and introduce two indices, the polarization difference and the angular difference, to avoid the dependence of the brightness temperature on the sea-ice thickness. They use a Maximum Likelihood Estimator in combination with these two indices in opposite to the more usual method of linear estimation used in algorithms designed for higher frequencies. They find that the retrieved SIC compare well with observations, except in fall, where there are differences in regions of thin ice due to the high penetration depth of the low-frequency radiation.

The topic is timely and the approach of the Maximum Likelihood Estimator is interesting. The authors took well into account previous comments and therefore improved the manuscript notably. However, I think there is still room for improvement in the structure and writing style. The clarity of your message would profit from a careful structure- and writing-oriented (instead of topic-oriented) proof-reading.

I suggest minor revisions. I have some comments and questions and I hope the authors can answer them. Also, I have some suggestions that could improve the clarity of the manuscript.

Authors: We thank the reviewer for his/her comments have helped improve the manuscript.

Thematic comments:

#1 It is not totally clear to me what is the advantage of this new method, with which I mean a SIC retrieval at 1.4 GHz. I can understand that there has not been any SIC retrieval at this frequency before but is it then not only one new method amongst others to retrieve SIC? If I understood right, this retrieval yields smaller errors in summer. You could underline a bit more that this is a

key advantage compared to other algorithms, which have problems in summer due to melt ponds and wet snow for example.

Authors: We feel the manuscript already addresses some key advantages of using L-band observations, which Fig. 1 captures visually, and an MLE optimization approach. These include the negligible effect of the atmosphere on the L-band measurements, its lesser sensitivity to temperature changes relative to radiometers that operate at higher frequencies, or the lack of any significant effect of snow depth on Tb V-pol measurements. Furthermore, Reviewer#3 made a valid point, the prospect that a new independent method affords to cross-check SIC results obtained with other methods. Moreover, as rightly pointed out by this reviewer, we expect this method to be better suited to SIC estimation during the wet summer months than others that are not based on L-band measurements. Quantifying this last statement would however require a comprehensive analysis including the construction of a match-up, quality-controlled database of optical imagery. This is beyond the scope of this study, and we leave it for future work.

A discussion on that point is added in the Conclusions section, in lines 627-635, page 19.

#2 On the same note, you state as an advantage that, as we now could in principal retrieve both sea-ice thickness and SIC from 1.4 GHz-measurements, these could be combined to retrieve both at the same time. But can thickness and concentration be retrieved at the same time if the retrieval method for SIC has problems in the thin ice areas (under 60 cm) and the retrieval method for sea-ice thickness is only for thin ice areas, up to 50 cm (Kaleschke et al., 2012; Huntemann el al., 2014)? I would like the authors to comment on that.

Authors: It feels that it should be possible to estimate SIC and SIT simultaneously thanks to the multi-angular observational feature of SMOS and the availability of two polarization. Although we had originally included this statement to motivate such a study, we have now removed it to only present the facts, and to steer clear from any controversy that an unsubstantiated hypothesis might carry. Still, we believe this would be a very important result, and we plan to pursue such study in the future.

Writing comments:

#3 The words "below", "above", "former", "latter" are used a lot. Often this is too vague and it is not clear what exactly is meant by them. The reader is pointed in a lot of directions and gets off the track of the actual message. I suggest that you rethink the structure of the manuscript to avoid as much as possible having to point to another place in a manuscript.

Authors: We thank the reviewer for his/her stylistic critique, to which we have tried to accommodate by forgoing those adverbs and adjectives when inessentials, and in several

other ways. We hope that the style and flow of the manuscript has thus improved, and that grammatical errors have also been resolved. And we obviously leave for TC copy-editing to ensure its consistency with the overall TC style.

#4 It is sometimes unclear what was done in the study and what has been done before. As you use several tenses (past, perfect, present, future) and active and passive mode in an inconsistent way (sometimes changing in the middle of a paragraph), I suggest to carefully proof-read the manuscript and and to correct the inconsistencies. This would remove some of the confusion.

Authors: Thank you, ditto.

#5 Also, very often a paragraph or sentence starts with "the figure shows", "the table shows" or "the authors show". I think if the emphasis was on the message of the figure/reference and the figure/reference was only given in parenthesis at the end of the sentence, your message would gain in clarity.

Consider as an example the difference between:

P13 L1-4 : "Figure 11 shows the spatial distribution of SIC in the Arctic Ocean estimated from (a) SMOS for the 3-day period 2–5 March 2015, (b) OSI-SAF SIC on 4 March 2014, and (c) the difference between (b) and (a). "

P14 L22-23 : "However, the sensitivity of the brightness temperature to sea surface temperature, atmosphere, and wind speed is clearly reduced when observing the sea surface with radiometers working at lower frequencies (Figure 1) ..."

Authors: Ditto. However, besides the stylistic approach, the level of complexity that figures convey can be markedly different. Some, like Figures 11, require an introduction to what is being shown before the message(s) can be given while others, like Figure 1, are more of the single-sentence message type.

#6 I find it confusing when parentheses are used for a whole sentence. Either it is important for the study, then the sentence can be written as such, or it is not important and it can be left out.

Authors: Ditto.

#7 Some sentences are very long with several dependencies and often too many or too less commas. I lost track several times. Shorter sentences would improve clarity.

Authors: Ditto.

#8 There are still several typos and grammatical mistakes. I tried to highlight some of them but I suggest that you let a native speaker or just another person read through your manuscript.

Authors: **We thank again the reviewer for his/her careful review and comments. We have tried our best to accommodate them, and we hope as a result the readability of the manuscript has improved.**

Specific Comments:

P1 L11: I don't see the logical connection from the previous sentence to the "therefore"

Authors: **Done**

P1 L18: Replace "ice cover" by "sea-ice cover"

Authors: **Done, in line 25, page 2**

P2 L5-7: The sentence is unclear as you use both "therefore" and "because". Try to divide it in to two sentences.

Authors: **Done, lines 49-45, page 2**

P2 L7 : Replace "since" by "for"

Authors: **Done**

P2 L16 : Comma after "that" and it is not clear to what "former" refers. Add "the ice penetration of the former".

Authors: **Done, lines 56, page 2**

P2 L22: I think you can leave out "what is left for a future work"

Authors: **Done**

P2 L29: Not clear why the spatial resolution of 35 to 50 km is a key feature. Maybe remove "key" in L28.

Authors: **Done, line 71, page 3.**

P3 L10: Remove the sentence in parentheses.

Authors: **Done**

P3 L30-31: Move the product version to the OSI SAF parenthesis.

Authors: **Done**

P4 L3 and L7 : I think you can remove "see below".

Authors: **Done**

P4 L5 : You always only mention data from 2014. Would it be right to only write "from the year 2014"? And then you could leave out in the rest of the manuscript all the time you mention "over the year 2014". If you use more years (that did not become clear to me), write "from 2014 to XXXX". Otherwise it is not clear when your data period ends.

Authors: **Done, line 125, page 4.**

P4 L13 : Remove "As discussed in Section 1"

Authors: **Done**

P4 L13 : Replace "different incidece angle at" by "different incidence angles to"

Authors: **Done**

P4 L14: I think you can start a new sentence: "TB can be expressed as".

Authors: **Done**

P4 L18: Replace "into" by "on"

Authors: **Done**

P4 L21: Write sentence without parentheses. Do you mean "We use TB to refer to surface brightness temperature"? The surface emissivity would be e_s, right? This is not clear.

Authors: **Done, line 144, page 5.**

P5 L4-5: There is no logical sequence between "varies linearly with emissivity" and "The nonlinearity".

Authors: **Done, we have deleted the nonlinearity sentence, line 155, page 5.**

P5 L7: Replace "with" with "on the"

Authors: **Done**

P5 L8-10: Write the sentence without parentheses

Authors: **Done. In fact the sentence has been changed considerably, line 145, page 5**

P5 L20: I think you can remove the sentence in parentheses.

Authors: **Done**

P5 L30: I think it would be clearer to introduce the equation directly when you cite it for the first time (near L8). Maybe it would work if you change the sequence of the paragraphs on P5 and P6.

Authors: Done. Now Eq. 5 is not cited before Eq. 4. We prefer not put Eq. 4 when we cite in the first time (line 174. Pg 6), since other assumptions and terms need to be defined before presented this equation.

P6 L25-29: I think this sentence is too long.

Authors: These are several sentences. We don't think that cutting it is necessary.

P7 L2: I think "microwave remote sensing model" is not the right term here. Maybe you mean "microwave emission model"?

Authors: Correct, done in line 254, pg 8.

P7 L10: Remove "deletedwhen"

Authors: Done

P7 L9-11: I don't understand this sentence.

Authors: Removed, it was not essential and was adding confusion.

P7 L20: It is not clear what "the former" refers to.

Authors: Indeed, now clarified as "the V-pol", Line 274, page 9.

P7 L24-29: "In this study","in this context","in this applications". The logical sequence of these sentences is not clear.

Authors: The three sentences have been rephrased to improve readability (see Line 285-290, pàge 9)

P8 L1: you could cite (Tab. 1) after ice

Authors: Done (line 294, page 9)

P8 L6: "indicated above" is not specific enough, it could be 25°, 60°, 30°, 50°.

Authors: Clarified as sigma = 50º and sigma = 25º, in line 300, page 10.

P8 L28: I don't know if "reasonable" is the right word here. Maybe "average"?

Authors: Reasonable is a better description, average would not be correct.

P9 L5: "done by other authors". It is not clear to what "done" refers. Did they focus on TB or on inversion algorithms using PD and AD? I am quite sure that it is the former but this is not clear from the sentence structure.

Authors: Indeed, they focussed on TB. But, in the new version the reference has been deleted, since it has been already explained before. (line 344, page 11)

P9 L14: If the level of uncertainty is unquantified, does it still mean that it is negligible?

Authors: No, it is not negligible, but it means that the error is not known. We have removed the word "unquantified." (line 354, page 11)

P9 L27: add "defined" before "above"

Authors: Done

P9 L32-P10 L2: The paragraph starts with "Table 1 lists". It reads as if you were introducing something new. But, actually, you have referenced Table 1 several times before. This relates again to the structural issue (see #3).

Authors: Edited the sentence (line 378, page 12). However, the focus of this sentence is different from the sentences in live 358 which also cite Table 1.

P11 L5: If possible, try to use another letter for the distributions. rho was already used for the density before.

Authors: The reviewer is right. We have changed rho by f in Eqs. 15 and 16.

Section 5.1.: This is more a listing of different figures than a coherent story (see #5). I suggest that you rethink about the message you want to convey in this section.

Authors: Section edited for improve readability and flow.

P12 L1: Remove "replacedmoenths" and replace "epochs" by "periods".

Authors: Done

P12 L29: I think you can remove "As we have shown"

Authors: Done in line 480, p 15.

P13 L5: I think you can remove "here" and "some days in"

Authors: Done

P13 L9: It is not clear to what "that response" relates to.

Authors: **Done in line 507, page 16.**

P13 L31-33: Reformulate this sentence. Not clear

Authors: **Done in 529, page 16.**

P14 L6: I think you can replace "that is, the square of correlation coefficients" by "R^2" or "r^2"

Authors: **Adopted in 567, page 17.**

P14 L11: You don't need to put parentheses here

Authors: **Done**

P14 L19: It is not clear if this has been identified by Ivanova et al. (2015) or by someone else.

Authors: **Changed for clarification.**

P14 L30: You introduce the full names of AD and PD only later in the conclusions (P15 L6).

Authors: **The acronyms PD and AD are defined where they first appear, in Sect. 4.1. They had been re-defined here to make the conclusion self-contained. We have no preference, leaving it to TC style.**

P15 L24: Do you mean "determination" or "correlation" coefficients?

Authors: **Determination.**

Figures:

The caption often contains more explanations than are needed. And I think you do not need to reference in which part of the text the figure is discussed. So I think you can remove all "see XXX".

Authors: **Done.**

Figure 1: A similar sentence can be found in the text, I think you can remote it

Authors: **Done.**

Figure 10, 11 and 12: I suggest that you use different colorbars. This would improve the clarity of the figures. You could use blue-white-red for difference plots and blues or reds for absolute values.

Authors: **We have modified the color palettes of difference figures to improve highlighting of features, but we consider that our choice is quite appropriate for absolute value.**

Figure 11 and 12: Replace "3th" by "3rd"

Authors: **Done.**

Figure 14: In the colorbar, replace "SAF<0.9" by "Both<0.9".

Authors: **Done.**

References:

Several references are missing dois. In other cases, the format of the dois is not consistent, e.g. for Huntemann et al, 2014, Shokr et al., 2015 and many others.

Also sometimes, journal abbreviations are used, sometimes not.

Tonboe et al., 2016 is not a discussion paper anymore.

Ulaby et al., 2014: Replace "adn" by "and" Vant et al, 1978: A "T" is missing in the beginning of the title.

Authors: **All the references have been reviewed and corrected.**

Manuscript prepared for The Cryosphere
with version 2015/04/24 7.83 Copernicus papers of the LaTeX class copernicus.cls.
Date: 31 May 2017

EstimatingMeasuring sea ice concentration in the Arctic Ocean using SMOS

Carolina Gabarro[1], Antonio Turiel[1], Pedro Elosegui[1,2], Joaquim A. Pla-Resina[1], and Marcos Portabella[1]

[1]Barcelona Expert Center, Institute of Marine Sciences, ICM/CSIC, Passeig Maritim Barceloneta 39, Barcelona, Spain.
[2]Massachusetts Institute of Technology, Haystack Observatory, Westford, MA, USA.

Correspondence to: Carolina Gabarro (cgabarro@icm.csic.es)

Abstract.

We present a new method to estimate sea ice concentration in the Arctic Ocean using brightness temperature observations from the Soil Moisture Ocean Salinity (SMOS) satellite. The method, which employs a Maximum Likelihood Estimator (MLE), exploits the marked difference in radiative properties between sea ice and seawater, in particular when observed over the wide range of satellite viewing angles provided by SMOS. Observations at L-band frequencies such as those from SMOS (i.e., 1.4 GHz, or equivalently 21-cm wavelength) are advantageous for the remote sensing of sea ice because the atmosphere is virtually transparent at that frequency.

We find that sea ice concentration (SIC) is well determined, quantified as a 0.75 correlation – the average value over the entire Arctic during year 2014 – between SIC estimates obtained using the MLE method on L-band data and the method of the Ocean and Sea Ice Satellite Application Facility (OSI-SAF) on data from sensors such as the Special Sensor Microwave/Imager (SSM/I and SSMIS).~~We find that sea ice concentration is well determined (correlations of about 0.75) when compared to estimates from other sensors such as the Special Sensor Microwave/Imager (SSM/I and SSMIS).~~ We also find that the performance of the method decreases under thin sea ice conditions (ice thickness $\lesssim$0.6 m). This result is expected because thin ice is partially transparent at L-band thus causing sea ice concentration to be underestimated. We~~therefore~~ argue that SMOS estimates can be complementary to estimates of sea ice concentration ~~of both thick and thin sea ice~~ from other satellite sensors such as the Advanced Microwave Scanning Radiometer (AMSR-E and AMSR-2) or SSMIS, enabling a synergistic monitoring of pan-Arctic sea ice conditions.

1 Introduction

The Arctic Ocean is under profound transformation. The rapid decline in Arctic sea ice extent and volume that is both observed and modeled (e.g., Comiso, 2012; Stroeve et al., 2012) may have become the key illustration of change in a warming planet, but change is widespread across the

whole Arctic system (e.g., AMAP, 2012; IPCC, 2013; SEARCH, 2013). A retreating Arctic sea ice cover has a marked impact on regional and global climate, and vice versa, through a large number of feedback mechanisms and interactions with the climate system (e.g., Holland and Bitz, 2003; Cohen et al., 2014; Vihma, 2014).

The launch of the Soil Moisture and Ocean Salinity (SMOS) satellite, in 2009, marked the dawn of a new type of space-based microwave imaging sensor. Originally conceived to map geophysical parameters of both hydrological and oceanographic interest (e.g., Martin-Neira et al., 2002; Mecklenburg et al., 2009), SMOS is also making serious inroads in the cryospheric sciences (e.g., Kaleschke et al., 2010, 2012; Huntemann et al., 2014). Developed by the European Space Agency (ESA), SMOS single payload, called Microwave Imaging Radiometer using Aperture Synthesis (MIRAS), is an L-band (1.4 GHz, or 21-cm wavelength) passive interferometric radiometer that measures the electromagnetic radiation emitted by Earth's surface. The observed brightness temperature (T_B) can be related to moisture content over the soil and to salinity over the ocean surface (Kerr et al., 2010; Font et al., 2013), as can be used to infer sea ice thickness (Kaleschke et al., 2012) and snow thickness (Maaß, 2013; Maaß et al., 2015).

Sea ice concentration (SIC), defined as the fraction of ice relative to the total area at a given ocean location, is often used to determine other important climate variables such as ice extent and ice volume. SIC has ~~therefore~~ been the target of satellite-based passive microwave sensors such as the Special Sensor Microwave/Imager (SSM/I and SSMIS)~~AMSR-2 and SSMIS~~ and the Advanced Microwave Scanning Radiometer (AMSR-E and AMSR-2) for more than 30 years. SIC can be estimated due to the fact that~~because~~ the brightness temperature of sea ice and seawater are quite distinct. There exists a variety of algorithms to retrieve SIC from T_B observations tuned to those higher-frequency sensors, that is frequencies between 6–89 GHz (e.g., Cavalieri et al., 1984; Comiso, 1986; Hollinger and Ramseier, 1991; Smith, 1996; Markus and Cavalieri, 2000; Kaleschke et al., 2001; Shokr et al., 2008). Those algorithms present different advantages and drawbacks depending on frequency, spatial resolution, atmospheric effects, physical temperature, and others. See for example Ivanova et al. (2015) for a review of a sample of thirteen of those algorithms. Although some authors (e.g., Mills and Heygster, 2011a; Kaleschke et al., 2013) have recently explored the feasibility of SIC determination using an aircraft-mounted L-band radiometer, a method that extends satellite-based SIC retrievals down to L-band (i.e., SMOS) frequencies has been missing. We therefore set out to develop a new method, which we present here.

A significant difference between high-frequency and L-band microwave radiometry is that ~~, unlike the former, the~~ ice penetration at L-band~~of the latter~~ is non-negligible (Heygster et al., 2014). In other words, ice is more transparent (i.e., optically thinner) at low than at high microwave frequencies. As a consequence, the brightness temperature measured by an L-band antenna is not only emitted by the topmost ice surface layer but by a larger range of deeper layers within the ice. Thanks to that increased penetration in sea ice (about 60 cm depending on ice conditions), the SMOS L-band

radiometer is also sensitive to ice thickness (Kaleschke et al., 2012; Huntemann et al., 2014). ~~In fact, ideally one would want to estimate both SIC and sea ice thickness simultaneously [e.g.,][]Mills.2011, what is left for a future work~~.

Wilheit (1978) analyzed the sensitivity of microwave emissivity of open seawater to a variety of geophysical variables such as atmospheric water vapor, sea surface temperature, wind speed, and salinity as function of frequency (Figure 1). The figure illustrates that L-band (1-2 GHz) observations are in a sweet spot, with the effect of all variables but salinity being minimal around the SMOS frequency. The same authors also showed that the signature of multi-year (MY) and first-year (FY) ice overlap in the lower microwave frequencies, while this is not the case at higher frequencies.

We exploit some of SMOS ~~key~~ observational features in this study to develop a new method to estimate SIC. These include a combination of acquisition modes involving dual and full polarization, continuous multiangle viewing between nadir and 65°, wide swath of about 1200 km, spatial resolution of 35-50 km, and 3-day revisit time at the equator but more frequently at the poles. In particular, the multiangle viewing capability of SMOS is a noteworthy feature; it means that the same location on the Earth's surface can be observed quasi-simultaneously from a continuous range of angles of incidence as the satellite overpasses it. ~~The spatial resolution of about 35-50 km.~~

The new method we present in this paper uses SMOS brightness temperature observations T_B and a Maximum Likelihood Estimator (MLE) to obtain SIC maps in the Arctic Ocean. We describe SMOS data and a radiative transfer model for sea ice that allows us to compute its emissivity, in Sections 2 and 3, respectively. We then introduce the concept of tie-points and its sensitivity to different geophysical parameters to help with SIC retrievals via algorithmic inversion of SMOS data, in Section 4.1, 4.2, 4.3, and 4.4, and the MLE inversion algorithm, in Section 4.5. We then perform an accuracy assessment of SIC estimates using SMOS by comparing them to an independent SIC dataset, in Section 5, to close with a discussion and conclusions, in Section 6 and 7, respectively.

2 Data

2.1 SMOS data from the Arctic Ocean

Since its launch in 2009, ESA has been generating brightness temperature full-polarization data products from SMOS. In this study, we focus on the official SMOS Level 1B (L1B) product version 504 data north of 60° N from 2014 to estimate SIC.~~(The analysis of the entire SMOS dataset, which continues to be growing, is left for future work.)~~ The L1B data contains the Fourier components of T_B at the antenna reference frame (Deimos, 2010), from which one can obtain temporal snapshots of the spatial distribution of T_B (i.e., an interferometric T_B image) by performing an inverse Fourier transform. The T_B data are geo-referenced at an Equal-Area Scalable Earth (EASE) Northern hemisphere grid (Brodzik and Knowles, 2002) of 25 km on the side. The radiometric accuracy of individual T_B observations from SMOS is ~2 K at boresight, and it increases ~~to ~4.5 K~~ on the

Extended Alias Free Field-of-View (Corbella et al., 2011). Proceeding from L1B data, though computationally more demanding than the more traditional L1C data products, has several benefits. For example, it allows one to change the antenna grid from the operational size of 128x128 pixels to 64x64 pixels. As shown by Talone et al. (2015), the smaller grid is optimal in that it helps mitigate some of the spatial correlations between measurements that are present in the larger grid.

We correct T_B for a number of standard contributions such as geomagnetic and ionospheric rotation and atmospheric attenuation (Zine et al., 2008). The galactic reflection is not significant at high latitudes, and no correction was applied. We then filter out outliers (defined as those estimates that deviate by more than 3-σ from the mean value, where σ is the radiometric accuracy at the given point in the antenna plane) and filtered out T_B observations in regions of the field of view that are known to have low accuracy due to aliasing (Camps et al., 2005), Sun reflections, and Sun tails.

To lower the noise level, we averaged T_B measurements from both ascending and descending orbits over periods of 3 days, which thus define the time resolution of our SIC maps ~~, over each grid cell~~. We also averaged acquisitions in incidence angle binnings of 2°~~intervals~~. Since some incidence angles could be missing due to the SMOS acquisition feature and interferences, we use a cubic polynomial fit to interpolate T_B measurements to have the full range of incidence angles in each grid position. ~~to locations that might otherwise not have T_B estimates over the full range of incidence angles.~~

2.2 OSI-SAF and other sea ice data products

We use SIC maps from the database ~~(product version OSI-401a)~~of the Ocean and Sea Ice Satellite Application Facility (OSI SAF product version OSI-401a) of the European Organization for the Exploitation of Meteorological Satellites (EUMETSAT) for comparison with the products we are obtaining.

These are computed from brightness temperature observations from SSMIS at 19 and 37 GHz, are corrected for atmospheric effects using forecasts from the European Center for Medium Range Weather Forecasts (ECMWF), use monthly dynamic tie-points ~~(see below)~~, are available on polar Stereographic 10-km grid for both polar hemispheres, and include SIC uncertainty estimates (Tonboe et al., 2016). In this study, we used daily SIC maps in the Arctic Ocean from the OSI-SAF northern hemisphere products of the years~~ince~~ 2014.

We also used SIC estimates from ice charts generated from various sensors by the National Ice Center (Fetterer and Fowler, 2009) to identify regions of interests~~defined the region that will be used~~ to compute the 100% ice-tie-points. ~~(see below)~~

3 Theoretical model of sea ice radiation at microwave wavelengths

~~The goal of this study is to develop a method that allows us to estimate Arctic sea ice concentration at SMOS electromagnetic frequency. Our approach will be to first describe the theoretical framework for the radiation emitted by sea ice in L-band. We will then describe a procedure that is robust when the values of the physical parameters of the model are unknown, which is often the case.~~

~~As we discussed in Section 1,~~ Passive radiometers measure brightness temperature T_B at antenna frame with different incidence angle. T_B can be expressed as:

$$T_B = \Upsilon\,[T_{B_{SURF}} + T_{B_{ATM\_DN}}] + T_{B_{ATM\_UP}}, \tag{1}$$

where Υ is the atmosphere transmitivity, $T_{B_{SURF}}$ the ~~self- emitted~~ radiation emitted by the surface, $T_{B_{ATM\_DN}}$ the downward-emitted atmospheric radiation that gets scattered by the terrain in the direction of the antenna, and $T_{B_{ATM\_UP}}$ the upward-emitted atmospheric radiation.~~self-emitted upward radiation from the atmosphere. Focussing on~~ The surface emission is defined as:

$$T_{B_{SURF}}(\theta) = e_s(\theta)T, \tag{2}$$

where θ is the incidence angle relative to zenith angle, e_s the surface emissivity, and T the physical temperature of the radiation-emitting body layer. Hereafter, we will use T_B to refer to surface brightness temperature ~~emissivity~~, for simplicity.

The emissivity e and reflectivity Γ of a layer are related by $e = (1 - \Gamma)$. The reflectivity (sometimes also called R) is the ratio between~~of~~ reflected and incident radiation at the media boundaries for each polarization. Γ for horizontal H and vertical V polarizations~~and~~ can be calculated using Fresnel equations, which depend non-linearly on the dielectric constant (ε), and on the incident θ_i and refracted θ_t angles:

$$\Gamma_H(\theta) = \left| \frac{\sqrt{\varepsilon_1}\cos\theta_i - \sqrt{\varepsilon_2}\cos\theta_t}{\sqrt{\varepsilon_1}\cos\theta_i + \sqrt{\varepsilon_2}\cos\theta_t} \right|^2, \qquad \Gamma_V(\theta) = \left| \frac{\sqrt{\varepsilon_2}\cos\theta_i - \sqrt{\varepsilon_1}\cos\theta_t}{\sqrt{\varepsilon_1}\cos\theta_t + \sqrt{\varepsilon_2}\cos\theta_i} \right|^2. \tag{3}$$

The frequency-dependent dielectric constant of a medium is a complex number defined as $\varepsilon(f) = \varepsilon^{'}(f) + i\varepsilon^{''}(f)$, where the real part $\varepsilon^{'}$ is related to the electromagnetic energy that can be stored in the medium, and the imaginary part $\varepsilon^{''}$ is related to the energy dissipated within the medium, and f is frequency. Note that brightness temperature varies linearly with emissivity (Eq. 2), hence also with~~on the~~ reflectivity. ~~The nonlinearity is an advantageous property for remote sensing that can be exploited by the multi-angle viewing capability of SMOS.~~

~~To calculate e_s, we will assume a sea ice model consisting of horizontal layers of three media – air, snow, and thick ice. We will use the incoherent approach (i.e., conservation of energy, instead of wave field treatment in the coherent approach) and the radiative transfer equation [e.g.,][]Burke.1979 to compute the net emission from the third and second media (i.e., ice and snow, respectively) into the first medium (i.e., air). The approach is similar to that used by other authors~~

~~Figure 2 shows the dependence of brightness temperature, with angle of incidence for seawater and sea ice, as well as that of ice overlaid by a dry snow layer (see Eq. 4 below), for nominal~~

~~Arctic temperature and salinity values. Specifically, temperature and salinity values used were after Maass.2013; for seawater −1.8°C and 30 psu, respectively, and for sea ice −10°C and 8 psu. Note that the T_B of seawater is significantly less than that of ice, and that the latter is slightly less than that of snow over ice. Also note the nonlinear dependence of T_B on incidence angle, the difference between horizontally (H) and vertically (V) polarized waves for all three models, and the higher larger variation with the incidence angle of H than that of V over ice and snow~

To calculate the brighness temperature T_B of sea ice, we will assume a sea ice model consisting of horizontal layers of three media – air, snow, and thick ice. We use the incoherent approach (i.e., conservation of energy, instead of wave field treatment in the coherent approach). Then a plane-parallel radiative transfer model (Eq. 4) is used to propagate to the surface the reflectivity computed at and through the ice-snow and snow-air media boundaries, and making a number of simplifying assumptions. Specifically, our model assumes (a) that the media are isothermal and (b) that the thickness of the ice layer is semi-infinite so that radiation from an underlying fourth layer (i.e., seawater) does not need to be considered. This approach is similar to that used by other authors (e.g., Mills and Heygster, 2011b; Maaß, 2013; Schwank et al., 2015). These assumptions are realistic for the ~~spontaneous~~ emission of sea ice that is thicker than about 60 cm at the observing frequency of SMOS, as discussed in Section 1, since the underlying seawater then makes no contribution to the overall emissivity. ~~(But see below for the case of thin ice.)~~

To further simplify our approach, we assume that the snow layer in the model consists of dry snow, which is typical of winter Arctic conditions. Dry snow can be considered a lossless medium at 1.4 GHz, due to the fact that the imagenary part of ε is very small compared with the real part, as stated in Schwank et al. (2015). That means that there is no attenuation in the snow layer, and therefore its attenuation coefficient, α_{snow}, is considered zero. We make this simplifying assumption because water in a wet snow layer would cause attenuation and therefore increase the total emissivity, but it is rarely possible to obtain meaningful data on the amount of water in wet snow. However, dry snow still has an effect on the refracted angle according to Snell's law, hence on the emissivity, which is computed via Eq. (3). ~~changes with the angle of incidence according to Snell's law.~~ The permittivity of dry snow depends on snow density (Tiuri et al., 1984; Matzler, 1996), which depend on the snow temperature. For a snow density of $\rho_s = 300\, g/cm^3$, the dry snow permittivity at L-band is $\varepsilon_{snow} = 1.53$ following the equation described in Schwank et al. (2015).

~~The brightness temperature of a thick-ice, dry-snow layered body that is measured at an angle of incidence θ with respect to the local vertical, polarization p, and observing frequency f can be simply calculated by propagating onto the surface the radiation that results from multiple reflections and refractions at the two media boundaries (i.e., ice-snow and snow-air) accounting for the infinite number of reflections between layers as Burke.1979:~~

We can now define the simplified brightness temperature that results from an infinite number of reflections between the three medias as (Ulaby et al., 1981):

$$T_B(\theta,p,f) = \left(\frac{1-\Gamma_{as}}{1-\Gamma_{as}\Gamma_{si}\exp^{-2\tau}}\right) \cdot \left[(1+\Gamma_{si}\exp^{-\tau})(1-\exp^{-\tau})T_{snow} + (1-\Gamma_{si})\exp^{-\tau}T_{ice}\right] + T_{sky}\Gamma_{as}, \quad (4)$$

where Γ_{as} and Γ_{si} are the reflectivity at the air-snow and snow-ice boundaries, respectively, and T_{snow} and T_{ice} are the physical temperature in the snow and ice layers, respectively. The term τ is the attenuation factor and is defined as $\tau = 2\,d\,\alpha\sec\theta$, where d is the depth of the snow layer and α the attenuation constant. T_{sky} is the temperature of the cosmic background. The dependence of T_B on θ, p, and f is embedded in the expressions of Γ and τ.

The attenuation constant α of the middle layer, in the case of a low-loss medium ($\varepsilon^{''}/\varepsilon^{'} << 1$), can be expressed as:

$$\alpha = \frac{\pi f}{c}\frac{\varepsilon^{''}}{\sqrt{\varepsilon^{'}}} \quad (5)$$

where c the speed of light. The skin depth is defined as $\delta_s = 1/\alpha$ (m) and characterizes how deep an electromagnetic wave can penetrate into a~~conducting~~ medium (e.g. Ulaby and Long, 2014).

~~The permittivity of dry snow is dependent on the snow density (Turi.1984, Matzler.1996). For a snow density of $\rho_s = 300\,g/cm^3$, the dry snow permittivity at L-band is equal to $\varepsilon_{snow} = 1.47$, with negligible imaginary dielectric constant. Therefore, the snow attenuation coefficient α_{snow} is considered zero at this frequency.~~

To compute the complex dielectric constant of sea ice ε_{ice}, which is needed to compute Γ_{si}, we use the classic empirical relationship by Vant et al. (1978). In this model, permittivity depends linearly on the ice brine volume V_b as,

$$\hat{\varepsilon}_{ice} = a_1 + a_2 V_{br} + i(a_3 + a_4 V_{br}) \quad (6)$$

where $V_{br} = 10\,V_b$, and the coefficients a_i can be obtained by linear interpolation to 1.4 GHz of the laboratory values from microwave measurements at 1 and 2 GHz (refer to Vant et al. (1978) for coefficient values).

The sea ice brine volume V_b can be computed using Cox and Weeks (1983) as follows:

$$V_b = \frac{\rho S}{F_1(T) - \rho S F_2(T)} \quad (7)$$

where ρ, S, and T are sea ice density, salinity, and temperature, respectively. The F functions are cubic polynomials derived empirically, namely

$$F_j(T) = \sum_{i=0}^{3} a_{ij} T^i \quad (8)$$

where the values of the coefficient a_{ij} were given in Leppäranta and Manninen (1998) for ice temperatures between –2 °C and 0 °C, and for lower temperatures in Cox and Weeks (1983); see also Thomas and Dieckmann (2003).

Figure 2 shows the dependence of brightness temperature, at L-band, with angle of incidence for seawater and sea ice, as well as that of ice overlaid by a dry snow layer (following Eq. 4), for nominal Arctic temperature and salinity values. Specifically, temperature and salinity values used were after Maaß (2013); for seawater –1.8°C and 30 psu, respectively, and for sea ice –10°C and 8 psu. Note that the T_B of seawater is significantly less than that of ice, and that the latter is slightly less than that of snow over ice. Also note the non-linear dependence of T_B on incidence angle, the difference between H- and V-polarized waves for all three cases, and the larger variation with incidence angle of H than V over ice and snow (e.g., Maaß et al., 2015).

We also calculate the theoretical emissivity e_s of a four-layer model using the Burke et al. (1979) equation. The additional layer in this model is the seawater under sea ice, and we use the dielectric constant of seawater from Klein and Swift (1977). This layer does not need to be considered for the case of (optically) thick ice~~described above~~, but it becomes "visible" for the case of (optically) thin ice (i.e., thicknesses $\leq$60 cm, depending on ice temperature and salinity). The expression of T_B for a four-layer model is defined in Burke et al. (1979) as:

$$T_B(\theta,p) = \sum_{i=1}^{3} T_i \cdot \left(1 - e^{(-\gamma_i(\theta)\Delta z_i)}\right) \cdot \left(1 + \Gamma_{p,i+1}(\theta) e^{(-\gamma_i(\theta)\Delta z_i)}\right) \cdot \prod_{j=1}^{i} [1 - \Gamma_{p,i+1}(\theta)] \cdot e^{(-\sum_{j=2}^{i} \gamma_{j-1}(\theta)\Delta z_{j-1})} \quad (9)$$

where T_i is the temperature of each layer, Γ its reflectivity, γ the absorption coefficient, and Δz the layer thickness. ~~Because the emissivity of seawater is significantly less than that of sea ice (Figure 2),~~ The net effect of reducing the sea ice thickness and starting to sense seawater, is ~~an overall~~ a decrease in surface emissivity, hence of T_B (as illustrated in Figure 5), relative to emissivity of thick ice (Shokr and Sinha, 2015).

4 Methods

4.1 Definition of robust indices from brightness temperature

It is rarely possible to obtain the ancillary geophysical data such as sea ice temperature, salinity, and ice thickness that is required to estimate brightness temperature from a microwave emission~~the microwave remote sensing~~ model.~~described above~~ Therefore, making assumptions and approximations becomes critically important ~~as discussed above~~. It is possible, however, to define a number of indices resulting from a combination of brightness temperature observations that are less sensitive to the unknown physical parameters. For example, estimates of soil moisture or sea ice concentration from radiometric measurements are often derived by combining T_B measurements obtained from different polarizations, frequencies, and angles of incidence (Becker and Choudhury, 1988; Owe et al., 2001). ~~Combinations of T_B measurements might result in lower sensitivity than that of~~

~~original T_B to the exact physical conditions, but good enough to distinguish among conditions such as phase changes, thus increasing robustness.~~

Hereafter, we use two indices, the polarization difference (PD) index and the angular difference (AD) index. The PD index is defined as the difference between T_B measurements obtained at vertical T_{B_V} and horizontal T_{B_H} polarizations as

$$\mathrm{PD}(\theta) = T_{B_V}(\theta) - T_{B_H}(\theta). \tag{10}$$

The AD index is defined as the difference between two vertical polarization T_B measurements obtained at two different angles of incidence as

$$\mathrm{AD}(\theta) = T_{B_V}(\theta + \Delta\theta) - T_{B_V}(\theta). \tag{11}$$

Figures 3 and 4 show the variation of PD and AD for the thick-ice model with angle of incidence, respectively. In defining AD, we use vertical rather than horizontal polarization because identification of the three media is facilitated by the larger dynamic range and non-crossing signatures of vertical polarization~~former~~ (Figure 4). We choose $\Delta\theta = 35^\circ$ angle difference because this value represents a good compromise between sensitivity of the index and radiometric accuracy in the case of SMOS (Camps et al., 2005) and, importantly, is also well supported by the wide range of satellite viewing angles that characterizes SMOS.

Although the Polarization Ratio (PR) is also a commonly used index, we have chosen PD after verifying that its dynamic range is larger than that of PR, and suspecting that PD would yield higher accuracy estimates given the SMOS error budget.

4.2 Calibration of sea ice concentration using tie-points

Tie-points are widely used for retrieving SIC with higher frequency radiometers, as well as in other fields such as photogrammetry (e.g., Khoshelham, 2009). In this study, we use tie-points as the typical T_B values for 100% and 0% concentrations which permit us to compute the~~ground-truth estimates of~~ sea ice concentration. ~~In this context tie-points are reference values of the two radiometric end-members for ocean pixels in the Arctic, that is, pixels that are completely covered by sea ice – 100% concentration – and pixels of open water – 0% concentration. In this applications,~~ Tie-points can therefore be viewed as SIC calibration points because their expected radiation can be unambiguously determined.

Figure 3 shows theoretical PD tie-point values for open water and sea ice, as well as ice with a snow layer. The values for an angle of incidence of 50° are marked by solid red circles. This angle represents a good compromise in PD contrast between the two media and SMOS accuracy (Camps et al., 2005). The two bounding values are 62.9 K for seawater and 26.8 K for ice with snow cover (Table 1). The large difference between tie-point values suggests that it is possible to estimate SIC at L-band.

Figure 4 shows theoretical AD tie-point values for difference in incidence angle $\Delta\theta = 35°$ and angles of incidence up to $\theta = 30°$ which, per Eq. 11, represents the T_{B_V} difference between $\theta = 60°$ and $\theta = 25°$. The values for an angle of incidence of 25° are marked by solid red circles, for which the tie-points are 51.8 K for seawater and 8.6 K for ice with snow cover (Table 1). Hereafter, PD and AD are evaluated at the incidence angles of $\theta = 50°$ and $\theta = 25°$, respectively. ~~indicated above.~~

Figure 5 shows that~~according the discussed 4-layer radiative transfer model~~ T_B at nadir increases non-linearly as function of ice thickness up to the saturation value of ~250 K, which is reached when ice becomes about 70-cm thick. Notice that ~~in the figure,~~ T_B estimates start at an ice thickness of 5 cm because there is a discontinuity in the Burke model as the thickness of ice tends to zero (e.g., Kaleschke et al., 2010; Mills and Heygster, 2011a; Maaß, 2013; Kaleschke et al., 2013).~~Also shown in Figure 5, theoretical AD and PD values for the incidence angles indicated above, as described by our model.~~ Compared with T_B, the total variation of both AD and PD with ice thickness is significantly smaller and, therefore, are better suited to estimate sea ice concentration.

4.3 Sensitivity of estimates of sea ice concentration to surface emissivity changes

In this section, we calculate the sensitivity of SIC estimates to changes in surface emissivity due to variations in the physical properties of sea ice (i.e., salinity, temperature, and thickness). We work with estimated SIC derived from the three indices~~parameters~~ T_B, PD, and AD. This is done following a standard error propagation method (as also used in Comiso et al. (1997)). It is important to determine how changes in ice conditions affect SIC estimates through those three indices to try to minimize SIC errors obtained using SMOS.

Table 2 lists the sensitivities, according to our theoretical model, of the indices I ($I = T_B$, PD, and AD) to the geophysical variables of ice and seawater: physical temperature (i.e., $\delta I/\delta T$), salinity ($\delta I/\delta S$), and thickness ($\delta I/\delta d$) evaluated within the ranges of T_{water}=[2,15], S_{water}=[10,38], T_{ice}=[-20,-5], and S_{ice}=[2,12]. It should be noted that those sensitivities are calculated using the model and the nominal Arctic temperature and salinity values defined in Section 3. In order to assess which index is less sensitive to changes in a given geophysical variable, we calculate absolute sensitivities, defined as the sensitivities multiplied by the dynamic range of the measurements.

Knowing the value of the tie-points of sea ice (SIC=100%) and seawater (SIC=0%), one can compute the average slopes of the SIC estimates to their corresponding parameters T_B, PD, and AD (i.e., $\delta SIC/\delta T_B$, $\delta SIC/\delta PD$, and $\delta SIC/\delta AD$). From data in Table 1, we obtain the average slopes as: $\delta SIC/\delta T_B = 0.65$, $\delta SIC/\delta PD = 2.32$, and $\delta SIC/\delta AD = 2.77$. These slopes can be used to propagate T_B, AD, and PD errors to errors in the SIC estimates.

We assume reasonable values for the variability of the physical parameters on which our emissivity model depends on, namely T, S and d of ice (generically denoted by g), as follows: ΔT=5 K, ΔS=4 psu, and Δd=30 cm. Using the values in Table 2 and the calculated average slopes~~above~~, one can finally compute the errors in SIC estimates associated with the geophysical variability of g when

the index I is used to evaluate SIC as:

$$\Delta SIC|_g = \left|\frac{\delta SIC}{\delta I}\right| \cdot \left|\frac{\delta I}{\delta g}\right| \cdot \Delta g \tag{12}$$

To evaluate the final impact of geophysical variability on the SIC evaluation using the index I, we compute the root-sum-squared (RSS) of the SIC uncertainties due to the geophysical parameters (Table 3). The table shows that AD is the most robust index to retrieve SIC, slightly better than PD, and significantly better than T_B. Because T_B is theoretically more sensitive to thin ice than the other two indices, one can expect that the use of T_B to retrieve SIC would result in larger SIC errors. Moreover, the uncertainty distribution of T_B is too broad, especially due to thickness, thus less adequate to fulfill the statistical hypotheses used to derive SIC. Despite the uncertainties in the theoretical physical model of ice, we consider the differences significant enough to focus on inversion algorithms using the PD and AD indices, and not on T_B. ~~as done by other authors e.g., Mills et al. 2011.~~

4.4 Comparison with empirical tie-points

Following the theoretical analysis~~above~~, we now turn to evaluate its performance empirically. We therefore select several regions of interest in the Arctic Ocean where SIC has been determined to be either 0% or 100% by other sensors and methods. To identify such regions, we use SIC maps from OSI-SAF and from the National Ice Center. In particular, we selected the open seawater region between latitudes 55°–70° N and longitudes 20° W and 25° E, which comprises more than 2000 pixels in a typical SMOS image. For sea ice, we selected the multi-year (MY) ice region between latitudes 78°–83° N (the northernmost latitude observable by SMOS) and longitudes 75°–150° W, which comprises about 1000 pixels per SMOS image. We expect some~~(yet unquantified)~~ level of uncertainty associated with the selection of the region to compute the 100% tie-points for summer periods stemming from known errors in the summer SIC products by OSI-SAF (Tonboe et al., 2016).

We calculated SMOS brightness temperatures of these target regions to evaluate their potential as empirical tie-points for seawater and sea ice. ~~Starting with T_B,~~ The temporal variation, in 2014, of the spatially averaged (median) T_B at nadir of the two geographic regions~~above~~ are shown in Figure 6. The values are consistent with the modeled values in Table 1. For the seawater region, the figure shows that the brightness temperature is constant, at about 99 K, to within ~2.5 K (one σ standard deviation) throughout the year. For the ice region, T_B is also stable during the non-summer months, but it drops by about 20 K during the summer season due to changes in surface emissivity associated with snow and ice melt and concurrent formation of meltwater ponds. The factor-two increase in formal error in summer relative to winter is also an indication of increased radiometric variability in surface conditions (as shown in Table 1).

Figure 7 shows that the temporal radiometric stability of the seawater region during 2014, and that of sea ice during the non-summer months, is also reflected in the AD and PD indices, as one would

expect. This suggests that a different set of tie-points during winter and summer periods could be beneficial for the quality of the SIC retrievals. On the other hand, the AD and PD tie-point values are very stable during winter and spring (November to June), indicating that values are robust to variations on physical temperature and that may not be necessary to compute tie-point values often (daily or monthly), as done with the OSI-SAF product.

Figure 8 shows a 2-D scatter plot of AD and PD indices for the two regions defined above during March (winter tie-point) and July (summer tie-point) 2014. The index values associated with seawater and with ice group form two well-differentiated clusters, which implies that the two types of regions can be clearly segregated using these indices. This is also true for the summer tie-points even though in this case the dispersion is larger and values are closer to sea tie-points, as expected following Figure 7.

~~Table 1 lists~~ The modeled (with snow and without) and observed TB, AD, and PD tie-point values for winter and summer 2014, and the standard deviation (σ) of the measurements are listed in Table 1. It is encouraging that most of the values are in agreement at about 2σ despite underlying model assumptions such as uniform sea ice temperature and specular ocean surface. Another important result is that the observed SMOS data is closer to the model when snow is considered.

4.5 Retrieval of sea ice concentration

The brightness temperature of mixed pixels, that is, ocean pixels partially covered by sea ice, can be expressed as a linear combination of the brightness temperature of ice and seawater weighted by the percentage of each surface type (e.g., Comiso et al., 1997):

$$T_{B_{mixed}} = C\,T_{B_{ice}} + (1-C)\,T_{B_{water}} \tag{13}$$

where C is the fraction of ice present in a pixel, with $C = 1$ corresponds to 100% of ice and $C = 0$ to 0% of ice, or equivalently 100% of seawater. Since AD and PD (Eqs. 10-11) depend linearly on brightness temperature, Eq. (13) can be used to express both AD and PD.

There are several possible strategies to estimate sea ice concentration at a given pixel from the AD and PD values measured at that pixel. The simplest approach is to consider that the values of the tie-points are good representatives of the values of AD and PD at the respective medium, i.e., seawater and sea ice, such that

$$\begin{aligned} \mathrm{AD} &\approx C\,\mathrm{AD}_{ice} + (1-C)\,\mathrm{AD}_{water} \\ \mathrm{PD} &\approx C\,\mathrm{PD}_{ice} + (1-C)\,\mathrm{PD}_{water} \end{aligned} \tag{14}$$

Concentration C can thus be retrieved from the value of either AD or PD by inverting the associated linear equation. In general, C can also be evaluated simultaneously with the AD and the PD observations by averaging the values obtained from both indices, as:

$$C = \frac{1}{2}\left[\frac{\mathrm{AD} - \mathrm{AD}_{water}}{\mathrm{AD}_{ice} - \mathrm{AD}_{water}} + \frac{\mathrm{PD} - \mathrm{PD}_{water}}{\mathrm{PD}_{ice} - \mathrm{PD}_{water}}\right] \tag{15}$$

This is known as the Linear Estimation of SIC. However, this approach might be too simple, as the values of AD and PD on ice and seawater can have some non-negligible dispersion due to geophysical conditions and to radiometric noise.

In this paper, a new inversion algorithm to estimate C is presented, which considers that AD and PD have known distributions, and by combining the observations it is possible to infer the value of C that is statistically more probable. ~~, given those observations.~~

The distributions of the SMOS AD and PD are unimodal and symmetric (not shown), thus allowing us to approximate them by Gaussians and considering the pure ice and pure sea measurements as independent. Therefore we can easily use a Maximum-Likelihood Estimation (MLE) approach. The MLE has many optimal properties in statistical inference such as (e.g., Myung, 2003) sufficiency (the complete information about the parameter of interest is contained in the MLE estimator), consistency (the true value of the parameter that generated the data is recovered asymptotically, i.e. for sufficiently large samples), efficiency (asymptotically, it has the lowest-possible variance among all possible parameter estimates), and parameterization invariance (same MLE solution obtained independent of the parametrization used).

Assuming the linearity superposition of indices (Eq. 14), it follows that the distributions of AD and PD (f_{AD},f_{PD}) in a general ocean pixel can be expressed as:

$$f_{\mathrm{AD}} \sim \mathcal{N}\left(C\,\overline{\mathrm{AD}}_{ice} + (1-C)\,\overline{\mathrm{AD}}_{water}, \sqrt{C^2\,\sigma^2_{\mathrm{AD}_{ice}} + (1-C)^2\,\sigma^2_{\mathrm{AD}_{water}}}\right) \tag{16}$$

$$f_{\mathrm{PD}} \sim \mathcal{N}\left(C\,\overline{\mathrm{PD}}_{ice} + (1-C)\,\overline{\mathrm{PD}}_{water}, \sqrt{C^2\,\sigma^2_{\mathrm{PD}_{ice}} + (1-C)^2\,\sigma^2_{\mathrm{PD}_{water}}}\right) \tag{17}$$

where the bar over the AD and PD indices refers to their mean values, the subindex identifies the medium, and σ is the associated standard deviation for each index and media. To obtain the mean and standard deviation values, we used the SMOS measurements at the regions for generating tie-points ~~regions~~ and periods discussed ~~above (see~~ in Sect. 4.4. The symbol $\mathcal{N}$ means normal probability density function.~~, that is:~~

As a first approximation, we have considered AD and PD two independent variables. It thus follows that the likelihood function $\mathcal{L}$ is equal to the product of their distributions or, equivalently

and conveniently, to their sum (recall that the likelihood is the logarithm of the probability density function), thus:

$$\widehat{l} = \ln(\mathcal{L}) = \ln(f_{AD}) + \ln(f_{PD}) \tag{18}$$

The MLE of SIC is the value of C that maximizes the likelihood function $\widehat{l}$.

5 Results

5.1 Quality algorithm assessment~~Internal consistency of SMOS SIC retrievals~~

We have calculated AD and PD values from SMOS brightness temperature and used the MLE approach ~~described above~~to obtain SIC estimates over the Arctic Ocean in year 2014. We have estimated SIC using different tie-points, characterized by their central value and dispersion. For seawater, we have used a single, year-round median value and the associated standard deviation for each index. For ice tie-points, we have used two sets of values, as suggested by the results in Figure 7. For the first set, we have computed for all years the median of the tie-points between December and May (Table 1), i.e., the winter-spring months when Arctic sea ice extent is close to its annual maximum. For the second set, we have used those same winter-spring values for the months of October through May but the average of the summer values for the months between June and September (Table 1). We have not used the October nor November data to compute ice tie-points values because these are months of maximum extension of thin ice, and underlying emission through thin ice could cause some errors on the SIC estimates (Figure 5 and Table 2).

~~Figure 9 shows The root-mean-square (RMS) error, relative to OSI-SAF, of SIC retrievals over the Arctic Ocean using four types of retrievals and two sets of tie-points.~~ The root-mean-square (RMS) error of SIC retrievals relative to OSI-SAF over the Arctic Ocean is shown in Figure 9. Four types of retrievals and two sets of tie-points are compared. Introducing a specific set of summer tie-points (black solid line) reduces the RMS error with respect to using only one unique tie-point for the whole year (black dotted line). The RMS reduction is about 24% and 12% in July and August, respectively, and to smaller degree in June and September. Therefore, we will hereafter use a different set of tie-points values in summer and winter.

Furthermore, using the set of summer-winter tie-points,~~leads to a significant reduction of the RMS error, relative to OSI-SAF,~~ results from four types of inversions that stem from combinations of linear and MLE method and indices are compared in Figure 9.~~The figure shows the results of the four combinations namely of linear and MLE method and the set of indices that allow to discriminate SIC, and either AD alone or AD and PD in combination.~~ The lowest RMS values through all months in 2014 but January are obtained with the MLE inversion algorithm and the AD index alone. The evolution along the year of the RMS obtained with the linear retrieval method is similar in the

case of the MLE method, but at ∼5-10% increased noise level. Larger RMS values and increased temporal variability are observed when the PD index is also used. The RMS error of all retrievals is largest in Fall, in particular if the PD index is used. Those are months of ice formation, therefore vast regions become covered with frazil ice, nilas, and thin young ice, following the minimum ice extension of September. All methods converge to similar results in September, since this period is the one with minimum ice extension and minimum thin ice is expected (so resulting in very small difference between using AD or AD and PD methods). ~~In the next subsection, a physical explanation and analysis of the behavior during Fall is given.~~

~~Figure 10 shows~~ The spatial variation of the difference in MLE SIC retrievals when using only the AD index and when using the AD and PD indices for the period 2–5 November 2014 is shown in Figure 10. As expected, the largest differences are associated with regions of thin ice formation, in particular in the Laptev Sea, Kara Sea, and along the edge of the ice pack both in the western Arctic and the Atlantic sector. Together, the spatio-temporal snapshots in Figures 9-10 highlight the sensitivity of PD to the presence of thin ice, what naturally leads to an increase of the retrieval error when PD is used. This conclusion is not fully consistent with the analysis done using the models in Section 4.3, on the dependence of the indices (T_B, PD, AD) on ice thickness. Table 2 shows that, theoretically, PD is slightly less sensitive to thin ice than AD. However, the AD index is the least sensitive (lowest RSS) to variations of all the analyzed variables. Therefore, we will hereafter use the AD index, summer-winter tie-points values, and an MLE-based estimator for SIC retrievals.

5.2 Accuracy assessment of SMOS SIC retrievals

~~As we have shown,~~ We have evaluated the mutual consistency of the SMOS SIC retrievals, and in the process we have determined which is the approach that leads to the minimum error in the retrieval of SIC. We now evaluate the accuracy of those retrievals. Although a representative (in the space-time domain) ground-truth dataset that allows us to assess the accuracy of SMOS retrievals does not exist, the SIC estimates from OSI-SAF ~~(already used above)~~ are a good option for cross-check. They are independent from SMOS, the spatio-temporal sampling and resolution of their products is commensurate with that of SMOS, and their error budget is available.

~~Figure 11 shows the spatial distribution of SIC in the Arctic Ocean estimated from (a) SMOS for the 3-day period 2–5 March 2014, (b) OSI-SAF SIC on 4 March 2014, and (c) the difference between (b) and (a). We have shown March because is the month of maximum sea ice extent, but the results for other months are similar. As explained, the largest differences between both algorithms are located at the margins of the sea ice cover, where thinner ice can be expected.~~

The spatial distribution of SMOS SIC in the Arctic Ocean has been estimated from SMOS data for the 3-day period 2–5 March 2014 and it has been compared with OSI-SAF SIC product on 4 March 2014 . The largest differences between both algorithms are located at the margins of the sea

ice cover, where thinner ice can be expected (see Figure 11). March is the month of maximum sea ice extent, but the results for other winter months are similar.

~~Figure 12 is the same as Figure 11 but in November, the month of maximum extension of thin young ice. Significant differences are now observed over a much wider area of the Arctic Ocean including the Barents, Kara, Laptev, East Siberian, and Beaufort seas. That is because thin ice is widely present in this season, and the radiometric response of SMOS to thin ice and the response of the microwave radiometers used by OSI-SAF are distinctly different.~~

On the other hand, November is the month of maximum extension of thin young ice, specially through the Beaufort Sea since ice in the Laptev and Kara seas remains thin during winter (Shokr and Dabboor, 2013). Significantly larger differences between SMOS and OSI-SAF products are now observed over a much wider area of the Arctic Ocean including the Barents, Kara, Laptev, East Siberian, and Beaufort seas (Figure 12).

~~That response is linked to the~~ The brightness temperature measured by a passive microwave radiometer, ~~which~~ increases with sea ice thickness up to a saturation value. Such an increase is more gradual for low frequencies and horizontal polarization (e.g., Ivanova et al., 2015). At the SMOS L-band, the increase of emissivity with ice thickness reaches saturation for an ice thickness that is about 60 cm, depending on ice salinity and temperature (Kaleschke et al., 2012) whereas at the OSI-SAF frequencies (19 and 37 GHz) is only a few cm (Heygster et al., 2014; Ivanova et al., 2015). ~~It is reasonable to infer that the observed SIC differences between SMOS and OSI-SAF are mainly associated with the different thickness of thin ice and ensuing penetration depths.~~ For example, for pixels that are 100% covered by thin ice of say 25-cm thickness, the AD and PD values for those pixels will be slightly different than the tie-point value of ice because the value of ice tie-points was computed from thick, MY ice (see Figure 5) for model analysis. This contrast leads to a difference in classification of such pixels, that will be considered mixtures of water and ice in the case of SMOS, and as 100% ice with OSI-SAF. In other words, the estimation of SIC of a seas covered by frazil ice and nilas will be higher for OSI-SAF than for SMOS.

To further analyze this classification difference, we have calculated the probabilities of SMOS SIC conditioned by values of OSI-SAF SIC using a full year, 2014, of Arctic-wide estimates. ~~Figure 13 shows (red) t~~The probability of estimating a SIC value with SMOS that is less or equal than 5% when the estimated OSI-SAF SIC is 0% is shown in Figure 13 (red line). As expected, the conditioned probability is very high throughout the year. This implies that both products have a similar ability to detect (close to) 100% ocean pixels. This implies that the probability of having high SMOS SIC values when OSI-SAF is low, is almost zero, which also means that the rate of triggering false alarms on ice detection with SMOS is low.

~~Figure 13 also shows (blue)the opposite situation, that is~~ On the contrary, the probability of estimating a SMOS SIC equal or higher than 90% while the OSI-SAF SIC is 100% is not constant during the year and decrease with respect to the previous case. During the winter period (between January

and April), the conditioned probability is notably high (near 0.9) (see Figure 13 blue line). Then it decreases sharply during spring and most notably in summer. This change in the conditioned probability starting in the spring could stem from a change in ice properties. ~~Ice properties change because~~As the snow becomes wetter with the onset of the melt season ~~in the spring~~ the observed emissivity starts to change, and this, varies with the observating frequency (different scattering response). ~~as well as differences in the retrieval algorithm. And regarding algorithms because OSI-SAF uses dynamically-adjusted tie-points (every 30 days) while the SMOS algorithms introduced here use two tie-points (summer and winter), what would explain the decrease of the conditioned probability.~~ The observed increase of the conditioned probability in June could be due to the use of a summer tie-point (applied from June to September) which improve the RMS with respect to OSISAF as shown in Figure 9. The low conditioned probability in Fall can be explained by the presence of thin ice.~~, as described above.~~

~~Figures 14 map the spatial distribution of the conditioned probability of SIC estimates for the months of March (a) and November (b). In the figures, the Arctic Ocean has been color-coded in three regions whereby both products have SIC above 0.9(red), OSI-SAF SIC is more than 0.9 while SMOS SIC is less than 0.9 (light blue) and OSI-SAF and SMOS SIC is less than 0.9 (dark blue). It becomes apparent that the light blue regions outline the edge of the ice cover, what is in good correspondence with the expected areas of thin ice.~~

We have analysed the spatial distribution of the conditioned probability of SIC estimates for the months of March and November. Those regions where OSI-SAF SIC is more than 0.9 while SMOS SIC is less than 0.9 (light blue color in Figures 14) outline the edge of the ice cover. This is in good correspondence with the expected areas of thin ice. Besides, this condition is extended when analysing November data (Figure 14b) when thin ice is more frequent in the Arctic.

~~Figure 15 shows the monthly spatial coefficients of determination (that is, the square of the correlation coefficients) between SMOS and OSI-SAF SIC throughout 2014. Because the values of SIC tend to be either 0 or 1 over wide Arctic regions, we have excluded both extremes from the figure as this would lead to too high, non-significant values of correlation. Thus, we have only included SIC values between 0.05 (5%) and 0.95 (95%) when computing correlations. During the winter months, the determination coefficient is high (more than 0.65), what again is consistent with our interpretation about the role of thin ice in SMOS SIC (during winter thin ice is scarce and is present only at the edge of the ice cover). As melt starts, the correlation between SIC estimates continues to be high, thanks to the summer tie-point. In September, ice cover extent is at minimum but because ice growth has not started yet there is almost no thin ice, and the correlation remains high. The correlation drops in the Fall (between October and December) because ice growth starts by freezing of the sea surface, producing large amounts of new thin ice.~~

During the winter months, the spatial coefficients of determination (r^2) between SMOS and OSI-SAF SIC is high (more than 0.65), what again is consistent with our interpretation about the role

of thin ice in SMOS SIC (see Figure 15). As melt starts, the correlation between SIC estimates continues to be high, thanks to the use of the summer tie-point in the retrieval. In September, ice cover extent is at minimum because ice growth has not started yet there is almost no thin ice, and the correlation remains high. The correlation drops in the Fall (between October and December) because ice growth starts by freezing of the sea surface, producing large amounts of new thin ice. To compute these values, we have only included SIC values between 0.05 (5%) and 0.95 (95%) when computing correlations to avoid the two extremes values leading to too high, non-significant values of correlation.

6 Discussion

The two PD and AD indices, which are derived from brightness temperature,~~Two indices derived from brightness temperature, the Polarization Difference (PD) and the Angular Difference (AD),~~ have been designed to maximize their differences between open water and sea ice. Both have a low response to changes in the geophysical characteristics of the media, which has been confirmed by using theoretical models and by performing sensitivity analysis.

The tie-points, defined as the characteristic values of our reference indices on the different media, have been calculated from SMOS data. When compared to theoretical values, some small discrepancies at the 10-20% level have been observed, probably due to simplifying assumptions such flat surface ice, flat sea, and constant temperature at the layers used in the theoretical models. We have thus decided to follow a more empirical approach. The use of two sets of tie-points, one for summer and one for winter measurements, improves the results of the summer SIC maps relative to a static unique tie-points. This improvement is not caused by changes in the ice or sea physical temperature, but most probably changes in the ice properties, because as snow and ice become wetter during the melt season, the observed radiometric emission changes. This effect is also observed on measurements from radiometers at higher frequencies than SMOS.

We have introduced the MLE inversion algorithm to retrieve SIC from SMOS data. The method is based on the maximization of the a posteriori likelihood of the joint distribution of AD and PD indices, assuming that they are independent and normally distributed. This MLE algorithm is more robust (less noisy) than the linear inversion (Eq. 14). It also improves the retrieved SMOS SIC with respect to a linear inversion method because the former takes into account the dispersion (error) of the tie-points (reference), which makes the algorithm more robust to T_B errors. SIC maps obtained using only the AD index are of better quality than when the AD and PD indices are used together. We attribute this to the higher sensitivity of PD than AD to physical changes in the media. ~~, as shown here both theoretically and empirically.~~

SMOS and OSI-SAF SIC maps compare well in terms of correlation (determination~~correlation~~ coefficient higher than 0.65) and RMS except in areas of thin sea ice. This difference can be ex-

plained by the higher penetration of SMOS in sea ice (about 60 cm) relative to the penetration from higher frequency radiometers. Thus, when ice is thinner than 60 cm SMOS data lead to lower values of SIC that OSI-SAF. ~~, what has been verified in this study. These results suggest that by combining SIC information from SMOS and OSI-SAF, one could potentially develop a mask for locations of thin ice.~~

7 Conclusions

According to Ivanova et al. (2015), the first source of error in the computation of sea ice concentration is the sensitivity to changes in the physical temperature of sea ice, in particular for those algorithms that use measurements between 10–37 GHz. They identify atmospheric water vapor and cloud liquid water ~~has been identified but they establish that it is the first source of error for those algorithms which uses the 89 GHz bands.~~ as the second source of error ~~especially for the presence of water vapor and cloud liquid water~~ except for algorithms at 89 GHz, where it becomes the dominant error. Another problem faced by higher frequency radiometers is that the SIC retrievals are affected by the thickness of snow cover, which is difficult to determine.

These authors also state that temporal variations in sea ice extent observed in the high-frequency radiometer data are also affected by atmospheric and other surface effects. For example, to compensate for the observed seasonal variations in ice tie-points of up to 10 K, they propose to dynamically obtain a new set of tie-points by using a running window of two-weeks length.~~These authors also state that the observed time trends in the measurements obtained by higher frequency radiometers are not only caused by trends in sea ice extent, but also by trends in the atmospheric and surface effects influencing the microwave emission measured by the satellite. Those authors observed seasonal changes on the ice tie-point of up to 10 K. In order to compensate those effects, they propose to dynamically derive the tie-points using a two-week running window; therefore, a new set of tie-points is defined regularly.~~

Estimating SIC using L-band observations such as those from SMOS is desirable because the effect of the atmosphere on brightness temperature is negligible, and the vertical polarization of T_B is insensitive to snow depth (Maaß et al., 2015). Moreover, AD and PD tie-point values have been shown to be very stable during winter and spring periods (Figure 7), indicating that the values are robust to variations in physical temperature. Thanks to that, one can safely assume two sets of static (i.e., not temporally varying) tie-points, one for each of summer and winter for SMOS data, and not fortnightly or monthly as is done in case of the OSI-SAF product. ~~However, the sensitivity of the brightness temperature to sea surface temperature, atmosphere, and wind speed is clearly reduced when observing the sea surface with radiometers working at lower frequencies (Figure 1), thus making SMOS more reliable and stable in those situations. Moreover, SMOS T_B is not affected by the snow thickness, as stated in Section 3.~~

~~Figures 6 and 7 show that SMOS PD, and AD have low sensitivity to surface physical changes, and present small trend, for the year observed, as shown in Figures 6 and 7. Thanks to that, one can safely assume two sets of static (i.e., not temporally varying) tie-points (summer and winter) for SMOS data.~~

SIC estimates from SMOS have some drawbacks with respect to those from higher-frequency radiometers. For example, whereas the spatial resolution of the high-frequency SIC estimates can reach ∼3 km, the resolution from SMOS will not be better than about 35 km. A second issue of SMOS is that it underestimates SIC in the presence of thin ice, which is characteristic of the ice edges and freeze-up periods. Therefore, SMOS data should be used in combination with some form of spatial masking for those regions. We suggest that SIC estimates from SMOS can complement those from higher-frequency radiometers, together yielding enhanced SIC products.

~~On the other hand, the best spatial resolution of SIC measurements with SMOS is about 35 km, which is low compared to the ∼3-km resolution that can be achieved with higher-frequency radiometers. Therefore, SMOS-based SIC estimates might be better suited for global climate studies.~~

~~An important problem that the retrieval of SIC with SMOS has to deal with is the underestimation of SIC values when thin ice (less than ∼0.60 m) is present, which are characteristic for the ice edges and freeze-up periods. Therefore this dataset is not accurate when thin ice is present and a mask should be used.~~

This dataset could be very beneficial during summer period, since SMOS SIC, theoretically, should be less sensitive to summer metamorphosis, due to the larger wavelength. Previous works show that the T_B and SIC measured at 6.9 GHz band are more robust to summer ice changes than higer frequency measurements (Kern et al., 2016; Gabarro, 2017). The confirmation of this statement will be done as future work.

~~The study presented here can be expanded in a variety ways, which we are currently exploring. For example, one could improve the quality of SIC maps by using more tie-points and better characterizing them over different spatial regions and for various times of year.One could also attempt to simultaneously estimate SIC and ice thickness (e.g. Rothrock.1988) over thin-ice regions by combining all the different SMOS observations acquired over the same point, thus providing independent estimates of ice volume over these regions. The study could also be further developed in the time-space domain since the present study has focused in a small fraction of the SMOS dataset making use of just four measurements from each pixel (two incidence angles and two polarizations), when more than 100 acquisitions can be obtained at each overpass.~~

Acknowledgements. This study has been funded by the National R+D Program of the Spanish Ministry of Economy through the Promises project ESP2015-67549-C3-R, as well as by previous SMOS-related grants.

References

AMAP: Changes in Arctic Snow, Water, Ice and Permafrost, Arctic Climate Issues 2011: Arctic Monitoring and Assessment Programme (AMAP), SWIPA 2011 Overview Report, Oslo, 2012.

Becker, F. and Choudhury, B. J.: Relative sensitivity of normalized difference vegetation Index (NDVI) and microwave polarization difference index (MPDI) forvegetation and desertification monitoring, Remote Sensing of Environment, 24, 297–311, doi:10.1016/0034-4257(88)90031-4, 1988.

Brodzik, M. J. and Knowles, K. W.: EASE-Grid: A versatile set of equal-area 0rojections and grids, Discrete Global Grids, 2002.

Burke, W., Schmugge, T., and Paris, J.: Comparison of 2.8- and 21-cm microwave radiometer observations over soils with emission model calculations, Journal of Geophysical Research, 84, doi:10.1029/JC084iC01p00287, 1979.

Camps, A., Vall-llossera, M., Duffo, N., Torres, F., and Corbella, I.: Performance of sea surface salinity and soil moisture retrieval algorithms with different ancillary data sets in 2D L-band aperture synthesis Interferometic radiometers, IEEE Transactions on Geoscience and Remote Sensing, 43, 1189–1200, doi:10.1109/TGRS.2004.842096, 2005.

Cavalieri, D., Gloersen, P., and Campbell, W.: Determination of sea ice parameters with the NIMBUS 7 SMMR, Journal of Geophysical Research, 89, 5355–5369, doi:10.1029/JD089iD04p05355, 1984.

Cohen, J., Screen, J. A., Furtado, J. C., Barlow, M., Whittleston, D., Coumou, D., Francis, J., Dethloff, K., Entekhabi, D., Overland, J., and Jones, J.: Recent Arctic amplification and extreme mid-latitude weather, Nature Geoscience, 7, 627–637, doi:10.1038/NGEO2234, 2014.

Comiso, J. C.: Characteristics of Arctic winter sea ice from satellite multispectral microwave observations, Journal of Geophysical Research, 91, 975–994, doi:10.1029/JC091iC01p00975, 1986.

Comiso, J. C.: Large Decadal Decline of the Arctic Multiyear Ice Cover, Journal of Climate, 25, 1176–1193, doi:10.1175/JCLI-D-11-00113.1, 2012.

Comiso, J. C., Cavalieri, D. J., Parkinson, C. L., and Gloersen, P.: Passive microwave algorithms for sea ice concentration: A comparison of two techniques, Remote Sensing of Environment, 60, 357–384, doi:10.1016/S0034-4257(96)00220-9, 1997.

Corbella, I., Torres, F., Duffo, N., Gonzalez-Gambau, V., Pablos, M., Duran, I., and Martin-Neira, M.: MIRAS Calibration and Performance: Results From the SMOS In-Orbit Commissioning Phase, IEEE Transactions on Geoscience and Remote Sensing, 49, 3147 –3155, doi:10.1109/TGRS.2010.2102769, 2011.

Cox, G. and Weeks, W.: Equations for Determining the Gas and Brine Volumes in Sea-Ice Samples, Journal of Glaciology, 29, doi:10.1017/S0022143000008364, 1983.

Deimos: SMOS L1 Processor Algorithm Theoretical Baseline Definition, SO-DS-DME-L1PP-0011, Tech. rep., Deimos Engenharia, 2010.

Fetterer, F. and Fowler, C.: National Ice Center Arctic Sea Ice Charts and Climatologies in Gridded Format, Version 1, http://dx.doi.org/10.7265/N5X34VDB, 2009.

Font, J., Boutin, J., Reul, N., Spurgeon, P., Ballabrera-Poy, J., Chuprin, A., Gabarró, C., Gourrion, J., Guimbard, S., Hénocq, C., Lavender, S., Martin, N., Martínez, J., McCulloch, M., Meirold-Mautner, I., Mugerin, C., Petitcolin, F., Portabella, M., Sabia, R., Talone, M., Tenerelli, J., Turiel, A., Vergely, J., Waldteufel, P., Yin,

X., Zine, S., and Delwart, S.: SMOS first data analysis for sea surface salinity determination, International Journal of Remote Sensing, 34, 3654–3670, doi:10.1080/01431161.2012.716541, 2013.

Gabarro, C.: The dynamical estimation of summer sea ice tie-points using low frequency passive microwave channels, OSI SAF Associated Visiting Scientist 16/03, OSISAF, EUMETSAT, 2017.

Heygster, G., Huntemann, M., Ivanova, N., Saldo, R., and Pedersen, L. T.: Response of passive microwave sea ice concentration algorithms to thin ice, in: IEEE Geoscience and Remote Sensing Symposium, pp. 3618–3621, doi:10.1109/IGARSS.2014.6947266, 2014.

Holland, M. M. and Bitz, C. M.: Polar amplification of climate change in coupled models, Climate Dynamics, 21, 221–232, doi:10.1007/s00382-003-0332-6, 2003.

Hollinger, J. and Ramseier, R.: Sea ice validation, in: DMSP Special Sensor Microwave/Imager Calibration/Validation, Tech. rep., Naval Research Laboratory, Washington, D.C, 1991.

Huntemann, M., Heygster, G., Kaleschke, L., Krumpen, T., Mäkynen, M., and Drusch, M.: Empirical sea ice thickness retrieval during the freeze up period from SMOS high incident angle observations, The Cryosphere, 8, 439–451, doi:10.5194/tc-8-439-2014, 2014.

IPCC: Climate Change 2013: The Physical Science Basis, Fifth Assessement, Tech. rep., Cambridge University Press, 2013.

Ivanova, N., Pedersen, L. T., Tonboe, R. T., Kern, S., Heygster, G., Lavergne, T., Sørensen, A., Saldo, R., Dybkjær, G., Brucker, L., and Shokr, M.: Satellite passive microwave measurements of sea ice concentration: an optimal algorithm and challenges, The Cryosphere, 9, 1797–1817, doi:10.5194/tc-9-1797-2015, 2015.

Kaleschke, L., Lupkes, C., Vihma, T., Haarpaintner, J., Bochert, A., Hartmann, J., and Heygster, G.: SSM/I Sea ice remote sensing for mesoscale ocean–atmosphere interaction analysis, Canadian Journal of Remote Sensing, 27, 5, 526–537, doi:10.1080/07038992.2001.10854892, 2001.

Kaleschke, L., Maaß, N., Haas, C., Hendricks, S., Heygster, G., and Tonboe, R. T.: A sea-ice thickness retrieval model for 1.4 GHz radiometry and application to airborne measurements over low salinity sea-ice, The Cryosphere, 4, 583–592, doi:10.5194/tc-4-583-2010, 2010.

Kaleschke, L., Tian-Kunze, X., Maaß, N., Mäkynen, M., and Drusch, M.: Sea ice thickness retrieval from SMOS brightness temperatures during the Arctic freeze-up period, Geophysical Research Letters, doi:10.1029/2012GL050916, 2012.

Kaleschke, L., Tian-Kunze, X., Maaß, N., Heygster, G., Huntemann, M., Wang, H., Hendricks, S., and Krumpen, T.: SMOS Sea Ice Retrieval Study (SMOSIce). Final Report, Tech. rep., ESA ESTEC Contract No.: 4000101476/10/NL/CT., http://icdc.zmaw.de/fileadmin/user_upload/icdc_Dokumente/SMOSICE_FinalReport_2013.pdf, 2013.

Kern, S., Rösel, A., Pedersen, L. T., Ivanova, N., Saldo, R., and Tonboe, R. T.: The impact of melt ponds on summertime microwave brightness temperatures and sea-ice concentrations, The Cryosphere, 10, 2217–2239, doi:10.5194/tc-10-2217-2016, 2016.

Kerr, Y. H., Waldteufel, P., Wigneron, J. P., Delwart, S., Cabot, F., Boutin, J., Escorihuela, M. J., Font, J., Reul, N., Gruhier, C., Juglea, S. E., Drinkwater, M. R., Hahne, A., Martin-Neira, M., and Mecklenburg, S.: The SMOS Mission: New Tool for Monitoring Key Elements ofthe Global Water Cycle, Proceedings of the IEEE, 98, 666–687, doi:10.1109/JPROC.2010.2043032, 2010.

Khoshelham, K.: Role of tie points in integrated sensor orientation for photogrammetric map compilation, Photogrammetric Engineering and Remote Sensing, 75, 305–311, doi:10.14358/PERS.75.3.305, 2009.

Klein, L. and Swift, C.: An Improved Model for the Dielectric Constant of Sea Water at Microwave Frequencies, IEEE Transactions on Antennas and Propagation, AP-25, 104–111, doi:10.1109/JOE.1977.1145319, 1977.

Leppäranta, M. and Manninen, T.: The brine and gas contents of sea-ice with attention to low salinities and high temperatures, Internal Report 2, Tech. rep., Finnish Institute of Marine Research, 1998.

Maaß, N.: Remote Sensing of Sea Ice thickness Using SMOS data, Master's thesis, Hamburg University, 2013.

Maaß, N., Kaleschke, L., Tian-Kunze, X., and T., R.: Snow thickness retrieval from L-band brightness temperatures: a model comparison, Annals of Glaciology, 56, doi: 10.3189/2015AoG69A886, 2015.

Markus, T. and Cavalieri, D.: An enhancement of the NASA Team sea ice algorithm, IEEE Transactions of Geoscience and Remote Sensing, 38, 1387–1398, doi:10.1109/36.843033, 2000.

Martin-Neira, M., Ribó, S., and Martin-Polegre, A. J.: Polarimetric mode of MIRAS, IEEE Transactions on Geoscience and Remote Sensing, 40, 1755–1768, doi:10.1109/TGRS.2002.802489, 2002.

Matzler, C.: Microwave permittivity of dry snow, IEEE Transactions on Geoscience and Remote Sensing, 34, 573–581, doi:10.1109/36.485133, 1996.

Mecklenburg, S., Wright, N., Bouzina, C., and Delwart, S.: Getting down to business - SMOS operations and products, ESA Bulletin, 137, 25–30, 2009.

Mills, P. and Heygster, G.: Retrieving ice concentration From SMOS, IEEE Geoscience and Remote Sensing Letters, 8, 283–287, doi:10.1109/LGRS.2010.2064157, 2011a.

Mills, P. and Heygster, G.: Sea Ice Emissivity Modeling at L-Band and Application to 2007 Pol-Ice Campaign Field Data, IEEE Transactions on Geoscience and Remote Sensing, 49, 612–627, doi:10.1109/TGRS.2010.2060729, 2011b.

Myung, J.: Tutorial on maximum likelihood estimation, Journal of Mathematical Psychology, 47, 90–100, doi:https://doi.org/10.1016/S0022-2496(02)00028-7, 2003.

Owe, M., Jeu, R., and Walker, J.: A Methodology for Surface Soil Moisture and Vegetation Optical Depth Retrieval Using the Microwave Polarization Difference Index, IEEE Transactions on Geoscience and Remote Sensing, 39, 1643–1654, doi:10.1109/36.942542, 2001.

Schwank, M., Mätzler, C., Wiesmann, A., Wegmüller, U., Pulliainen, J., Lemmetyinen, J., Rautiainen, K., Derksen, C., Toose, P., and Drusch, M.: Snow Density and Ground Permittivity Retrieved from L-Band Radiometry: A Synthetic Analysis, IEEE Journal of Selected Topics in Applied Earth Observations and Remote Sensing, 8, 3833–3845, doi:10.1109/JSTARS.2015.2422998, 2015.

SEARCH: Research, Synthesis, and Knowledge Transfer in a Changing Arctic: The Study of Environmental Arctic Change (SEARCH), Tech. rep., Arctic Research Consortium of the United States, 2013.

Shokr, M. and Dabboor, M.: Interannual Variability of Young Ice in the Arctic Estimated Between 2002 and 2009, IEEE Transactions on Geoscience and Remote Sensing, 51, 3354–3370, doi:10.1109/TGRS.2012.2225432, 2013.

Shokr, M. and Sinha, N.: Sea Ice. Physics and Remote Sensing, ISBN: 978-1-119-02789-8, AGU-WILEY, 2015.

Shokr, M., Lambe, A., and Agnew, T.: A new algorithm (ECICE) to estimate ice concentration from remote sensing observations: an application to 85-GHz passive microwave data, IEEE Transactions of Geoscience and Remote Sensing, 46, 4104–4121, doi:10.1109/TGRS.2008.2000624, 2008.

Smith, D.: Extraction of winter total sea-ice concentration in the Greenland and Barents Seas from SSM/I data, Internation Journal of Remote Sensing, 17, 2625–2646, doi:10.1080/01431169608949096, 1996.

Stroeve, J., Serreze, M., Holland, M., Kay, J., Malanik, J., and Barrett, A.: The Arctic's rapidly shrinking sea ice cover: a research synthesis, Climatic Change, 110, 1005–1027, doi:10.1007/s10584-011-0101-1, 2012.

Talone, M., Portabella, M., Martínez, J., and González-Gambau, V.: About the Optimal Grid for SMOS Level 1C and Level 2 Products, IEEE Geoscience and Remote Sensing Letters, 12, 1630–1634, doi:10.1109/LGRS.2015.2416920, 2015.

Thomas, D. and Dieckmann, G., eds.: Sea Ice. An Introduction to its physics, Chemistry, Biology and geology, Blackwell, 2003.

Tiuri, M., Sihvola, A., Nyfors, E., and Hallikaiken, M.: The complex dielectric constant of snow at microwave frequencies, IEEE Journal of Oceanic Engineering, 9, 377–382, doi:10.1109/JOE.1984.1145645, 1984.

Tonboe, R. T., Eastwood, S., Lavergne, T., Sørensen, A. M., Rathmann, N., Dybkjær, G., Toudal Pedersen, L., Høyer, J. L., and Kern, S.: The EUMETSAT sea ice climate record, The Cryosphere, 10, 2275–2290, doi:10.5194/tc-10-2275-2016, 2016.

Ulaby, F. and Long, D.: Microwave Radar and Radiometric Remote Sensing., University of Michigan Press, 2014.

Ulaby, F., Moore, R., and Fung, A.: Microwave Remote Sensing. Active and Passive, ISBN: 978-0890061916, Addison-Wesley Publishing Company. Advanced Book Program/World Science Division., 1981.

Vant, M., Ramseier, R., and Makios, V.: The complex-dielectric constant of sea ice at frequencies in the range 0.1–40 GHz, Journal of Applied Physics, 49, 1264–1280, doi:10.1063/1.325018, 1978.

Vihma, T.: Effects of Arctic Sea Ice Decline on Weather and Climate: A Review, Surveys in Geophysics, 35, 1175–1214, doi:10.1007/s10712-014-9284-0, 2014.

Wilheit, T. T.: A review of applications of microwave radiometry to oceanography, Boundary-Layer Meteorology, 13, 277–293, doi:10.1007/BF00913878, 1978.

Zine, S., Boutin, J., Font, J., Reul, N., Waldteufel, P., Gabarro, C., Tenerelli, J., Petitcolin, F., Vergely, J., Talone, M., and Delwart, S.: Overview of the SMOS Sea Surface Salinity Prototype Processor, IEEE Transactions on Geoscience and Remote Sensing, 46, 621 – 645, doi:10.1109/TGRS.2008.915543, 2008.

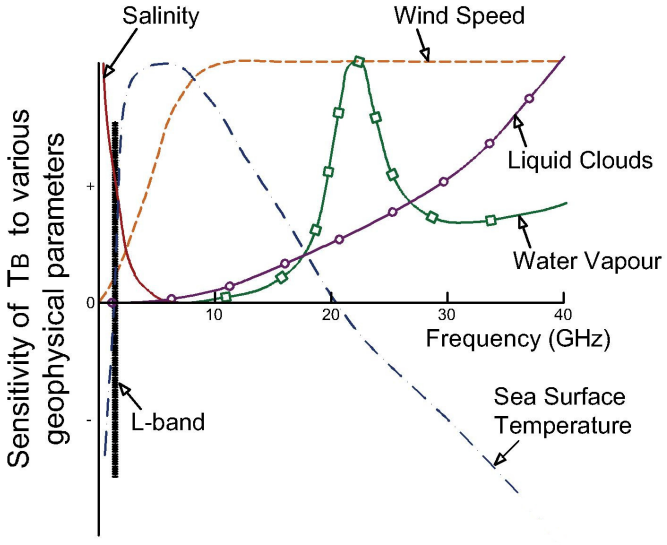

Figure 1. Sensitivity of brightness temperature for open seawater over a range of observing frequencies in the microwave band for a set of key geophysical parameters (created after Wilheit (1978) and Ulaby and Long (2014)). ~~The maximum sensitivity of T_B to sea surface temperature is around 6 GHz, with a peak of 0.4 $K/^\circ C$; to salinity is around 1 GHz, with a peak value of 0.5 K/psu; to wind speed is above 10 GHz, with a peak value of 1 K/m/s. The peak of attenuation from water vapor in clouds is at 22 GHz, and is 0.2 DB/km. L-band (1.4 GHz) observations are hardly sensitive to any variable but salinity, hence it is in a sweet spot for sea ice studies.~~

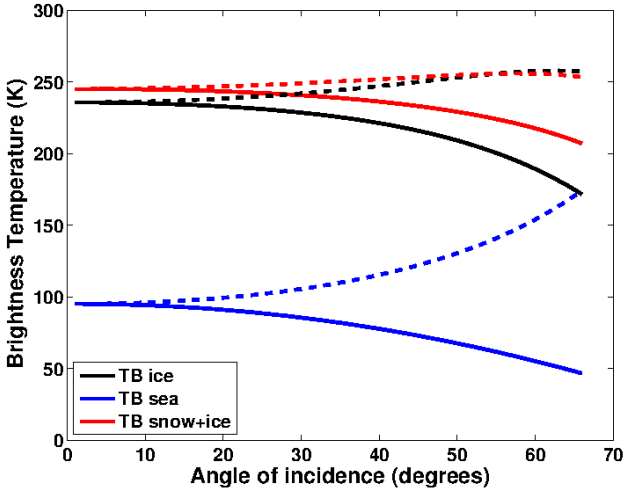

Figure 2. Theoretical variation of brightness temperature with angle of incidence at L-band for (blue) seawater, (black) sea ice, and (red) a snow layer overlying a sea ice layer for (continuous) horizontal and (dashed) vertical polarizations. ~~(See text in Sect. 3 for details.)~~

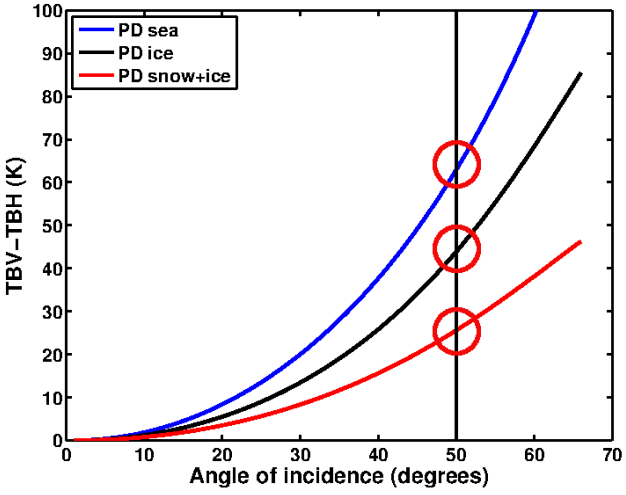

Figure 3. Modeled variation of polarization difference (PD) index with angle of incidence for (blue) seawater, (black) sea ice, and (red) a snow layer overlying a sea ice layer, at L-band. ~~(See Eq. 10 and text in Sec. 4.1 for details.)~~ The vertical line at 50° incidence angle is drawn for reference to tie-points, which are marked with a solid circle for the three media. ~~(see text in Sec. 4.2).~~

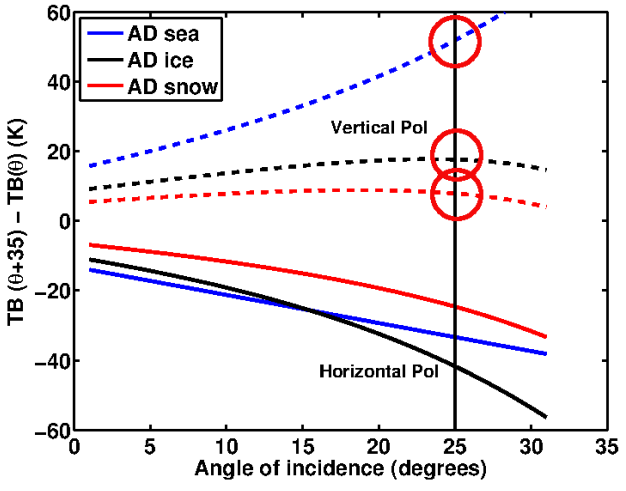

Figure 4. Modeled variation of angular difference index (AD) with angle of incidence for (blue) seawater, (black) sea ice, and (red) a snow layer overlying a sea ice layer for (continuous) horizontal and (dashed) vertical polarizations, and for $\Delta\theta = 35^\circ$, at L-band. ~~(See Eq. 11 and text in Sec. 4.1 for details.)~~ The vertical line at 25° incidence angle is drawn for reference to tie-points, which are marked with a solid circle on vertical polarization for the three media. ~~(see text in Sec. 4.2).~~

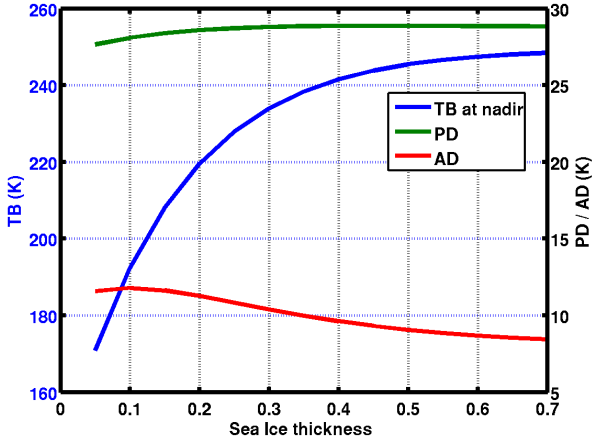

Figure 5. Theoretical variation with sea ice thickness of (blue; left axis) T_B at nadir, (green; right axis) polarization difference (PD) at 50° incidence angle, and (red; right axis) angular difference (AD) at $\Delta\theta = 25^\circ$ after the model by Burke et al. (1979), for a sea ice salinity of 8 psu, sea ice temperature of -10° C, and a snow layer of 10-cm thick over the ice. ~~(See text in Sect. 3 for details.)~~ Note the factor of 10 change between the left/right vertical scales.

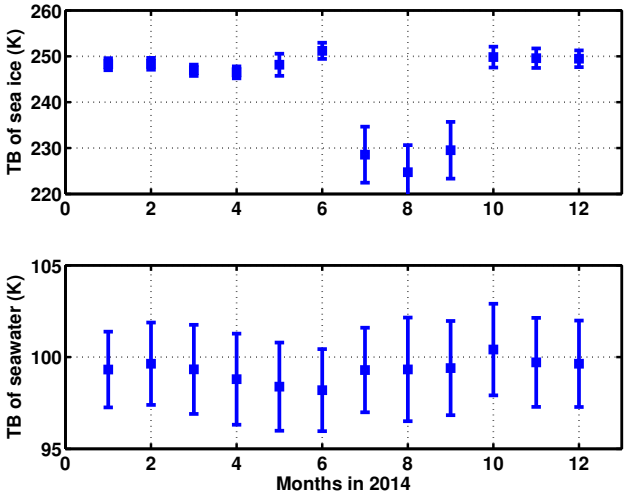

Figure 6. Temporal variation of the average brightness temperature T_B at nadir for (top) multy year sea ice and (bottom) seawater at the two regions for generating tie-points. ~~regions (see Sec. 4.4).~~Note the factor of 4 change in the vertical scales.

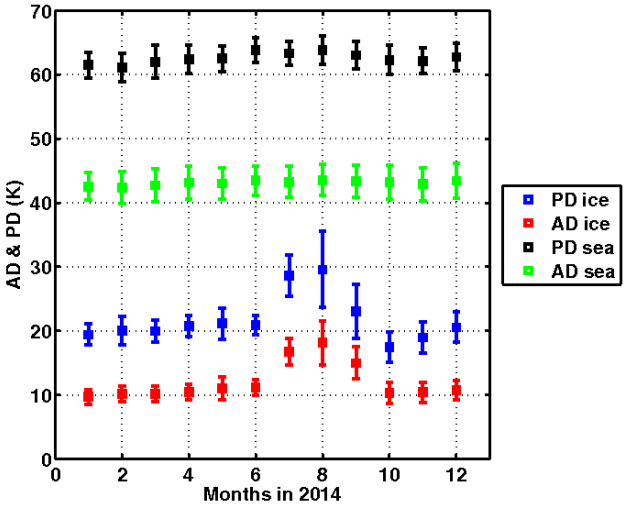

Figure 7. Same as Fig. 6 except here for angular and polarization difference indices.

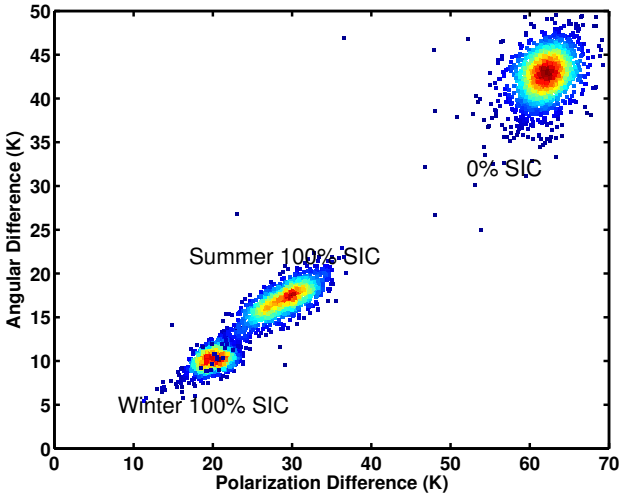

Figure 8. Scatter plot of the angular difference vs polarization difference in March and July 2014, with (red-to-blue) high-to-low index occurrence values for the two regions for generating tie-points ~~regions~~, i.e., 0% and 100% sea ice concentration (SIC).

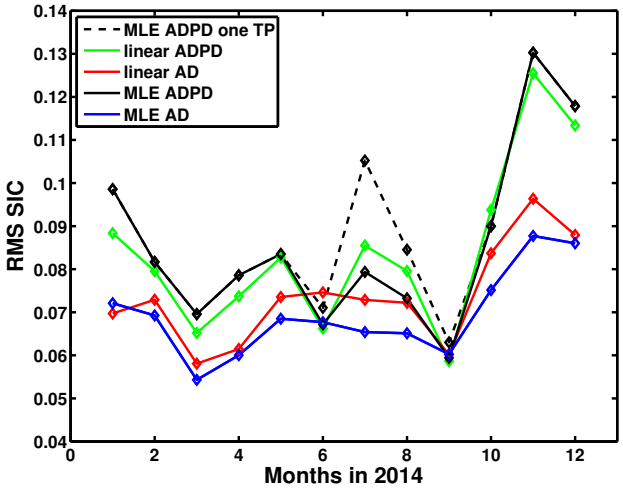

Figure 9. Comparison against OSI-SAF, of one tie-point (black dotted line) vs two tie-points (black plane line) with MLE; and MLE vs linear retrieval tecniques. If not defined in the labels it is two tie-points.

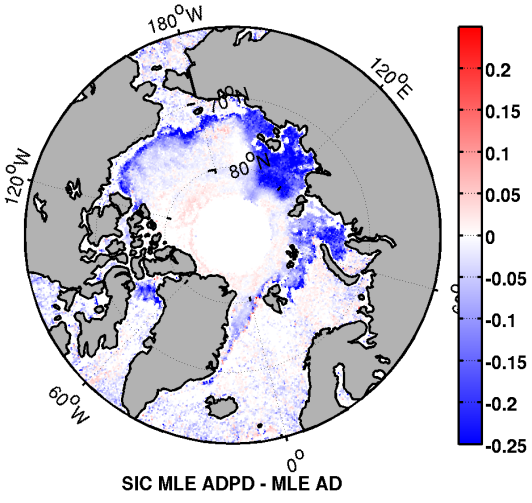

Figure 10. SMOS SIC with MLE AD+PD minus SMOS SIC with MLE AD inversion tecniques. SIC scale is presented from 0 to 1.

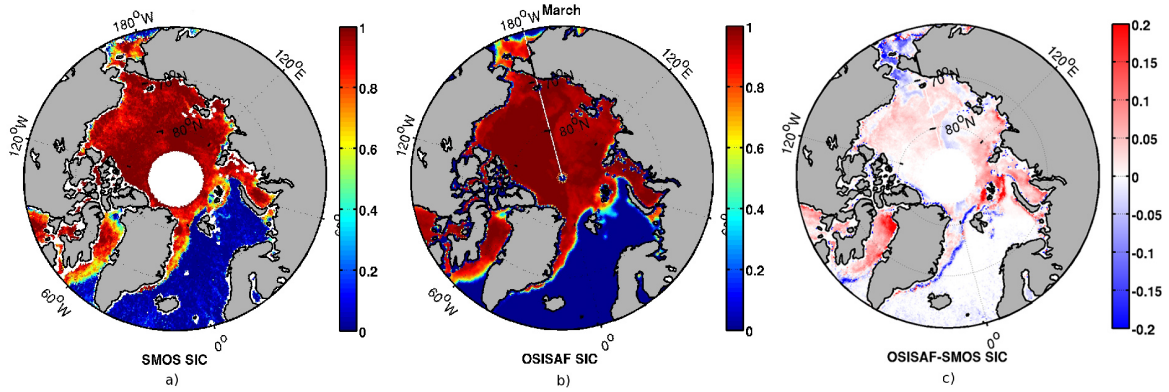

Figure 11. SMOS SIC with MLE (a), OSISAF SIC (b) and the differences (c) for 3rd March 2014.

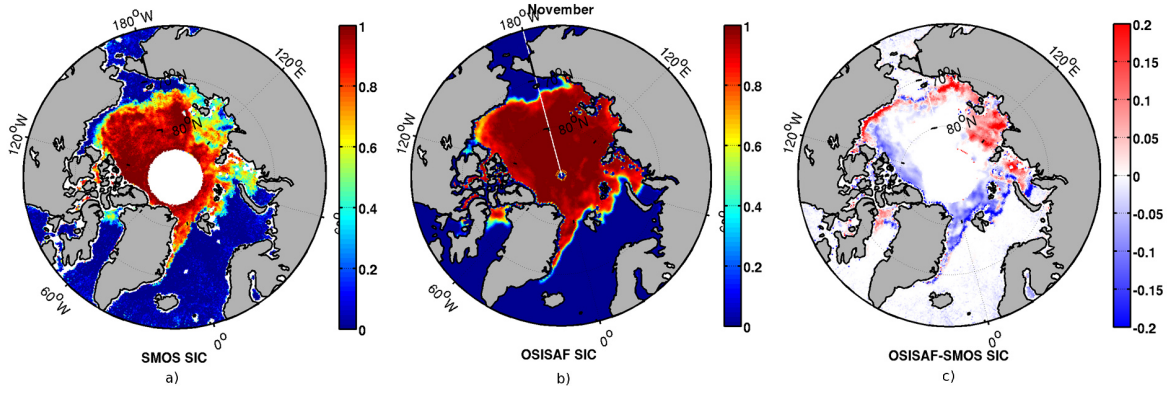

Figure 12. SMOS SIC with MLE (a), OSISAF SIC (b) and the differences (c) for 3rd November 2014.

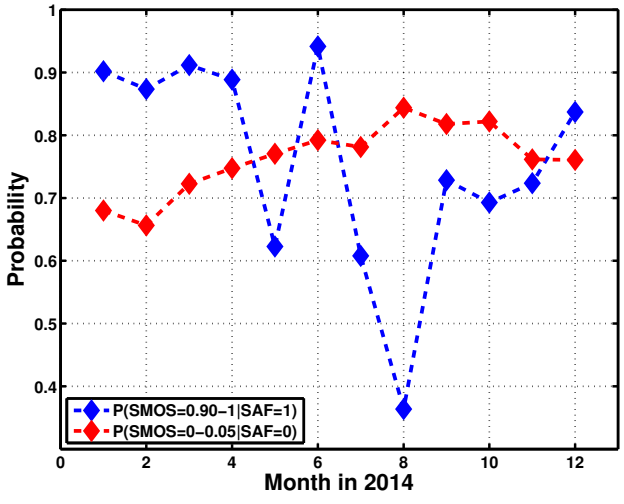

Figure 13. Probability to have SMOS SIC more than 0.90 where OSISAF SIC=1 (blue line) and SMOS SIC less than 0.05 where OSISAF SIC=0 (red line) for 2014. Summer tie-points are used for retrievals from June to September.

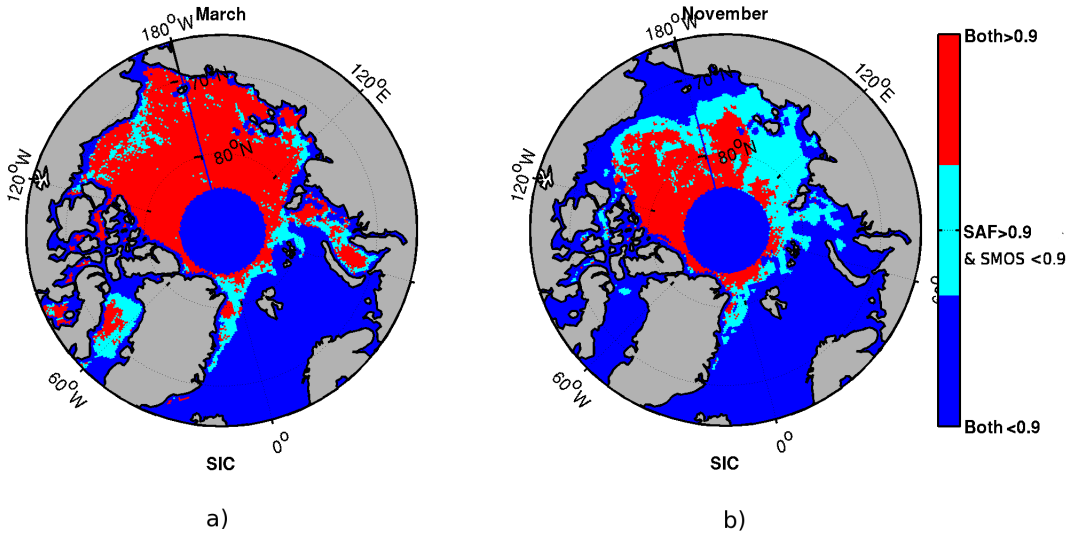

Figure 14. Classification of the Artic region according to their values of SMOS and OSI-SAF SIC during March (a) and November (b) 2014. Three classes are shown: 1) OSISAF $SIC < 0.9$; 2) OSISAF $SIC > 0.9$ and SMOS $SIC < 0.9$; and 3) OSISAF $SIC > 0.9$ and SMOS $SIC > 0.9$.

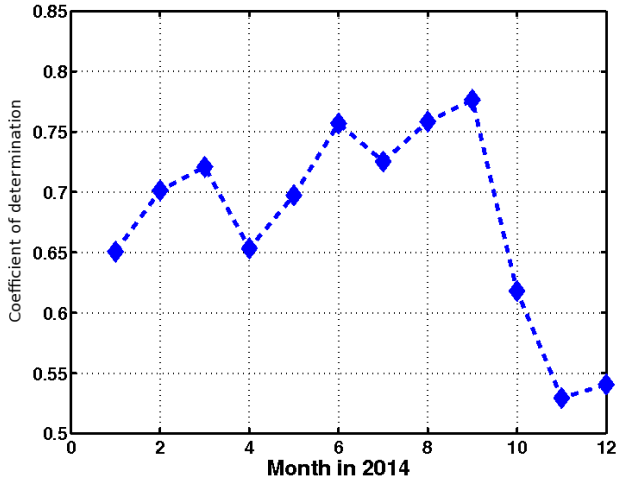

Figure 15. Coefficient of determination (R^2) between SMOS and OSISAF SIC for 2014, considering only SIC data in the range from 5% to 95%.

Table 1. Modeled (with and without snow) and SMOS observed T_B, PD, and AD median values. Errors quoted are the standard deviation around the median.

		Modeled (K)		Observed all year median $\pm\sigma$ (K)	
0% SIC (Seawater)	T_B	95.2		99.33 ± 2.40	
	PD	62.9		62.56 ± 2.56	
	AD	51.8		43.08 ± 2.57	
		Modeled with snow (K)	Modeled without snow (K)	Observed Winter median $\pm\sigma$ (K)	Observed Summer median $\pm\sigma$ (K)
100% SIC (Sea Ice)	T_B	249.2	239.3	248.21 ± 1.56	229.04 ± 4.99
	PD	26.8	45.9	20.30 ± 1.75	25.53 ± 3.72
	AD	8.6	18.8	10.38 ± 1.17	15.26 ± 2.31

Table 2. Sensitivity of measurement T_B, PD, and AD to ice temperature (T), salinity (S), and thickness (d).

Medium	Index (I)	$\delta I/\delta T$ (K /° C)	$\delta I/\delta S$ (K / psu)[1]	$\delta I/\delta d$ (K / cm)
Seawater	T_B	0.2	0.51	
	PD	0.26	0.21	
	AD	0.20	0.12	
Sea ice	T_B	0.85	1.00	1.2
	PD	0.66	0.35	0.02
	AD	0.35	0.25	0.05

[1] practical salinity units

Table 3. Propagated SIC error using each index, computed from Eq. 12 for assumed (T, S, d) variations, and root-sum-squared (RSS).

SIC error (%)	index used	ΔT 5 K	ΔS 4 psu	Δd 30 cm	RSS
ΔSIC	TB	2.8	2.6	23.4	23.7
ΔSIC	PD	7.6	3.2	1.4	8.3
ΔSIC	AD	4.8	2.8	4.2	7.0